Chlorophyll breakdown—Regulation, biochemistry and phyllobilins as its products

Hörtensteiner, Stefan ; Hauenstein, Mareike ; Kräutler, Bernhard

DOI: https://doi.org/10.1016/bs.abr.2019.03.004

Chlorophyll Breakdown - Regulation, Biochemistry and Phyllobilins as its Products

Stefan Hörtensteiner[a], Mareike Hauenstein[a] & Bernhard Kräutler[b]

[a] Institute of Plant and Microbial Biology, University of Zurich, Zollikerstrasse 107

CH-8008 Zurich, Switzerland

shorten@botinst.uzh.ch

[b] Institute of Organic Chemistry & Center for Molecular Biosciences (CMBI)

Innrain 80/82, University of Innsbruck, A-6020 Innsbruck, Austria

bernhard.kraeutler@uibk.ac.at

Abbreviations

ABA	abscisic acid
ABC	ATP-binding cassette
ACD	accelerated cell death
*bc*FCC	bicyclo-FCC
*bc*DFCC	bicyclo-DFCC
CBR	Chl *b* reductase
CCE	Chl catabolic enzyme
Chl	chlorophyll
Chlide	chlorophyllide
CYP	cytochrome P450 mono-oxygenase
DCC	dioxobilin-type (type-II) Chl catabolite
DFCC	dioxobilin-type (type-II) fluorescent Chl catabolite
DNCC	dioxobilin-type (type-II) nonfluorescent Chl catabolite
DPiCC	dioxobilin-type (type-II) pink Chl catabolite
DYCC	dioxobilin-type (type-II) yellow Chl catabolite
*hm*FCC	hypermodified FCC
FCC	fluorescent (type-I) Chl catabolite
HCAR	7^1-hydroxy Chl *a* reductase
HOChl *a*	7^1-hydroxy Chl *a*
*i*DNCC	*iso*-DNCC (an NDCC)
*i*PBon	isophyllobilanone
LHC	light harvesting complex
MES	methylesterase
*m*FCC	modified FCC
NCC	nonfluorescent (type-I) Chl catabolite
NDCC	nonfluorescent DCC
NMR	nuclear magnetic resonance (spectroscopy)
NOL	NYC1-like
NYC1	non-yellow coloring1
PAO	pheophorbide *a* oxygenase
PB	phyllobilin
*p*FCC	primary FCC
Pheide	pheophorbide
Phein	pheophytin
PiCC	pink (type-I) Chl catabolite
PPH	pheophytinase

*py*NCC	pyro-NCC
*py*Pheide	pyro-pheophorbide
RCC	red Chl catabolite
RCCR	RCC-reductase
*s*FCC	secondary FCC
SGR	stay-green (protein)
TIC55	translocon at the inner chloroplast membrane 55
UV/Vis	ultraviolet/visible (absorbance spectroscopy)
YCC	yellow (type-I) Chl catabolite

I Introduction

The appearance of the fall colors is a puzzling and fascinating phenomenon (Matile, 2000). The seasonally synchronized disappearance of chlorophyll (Chl) in autumn and the widespread re-greening of the vegetation in spring, are probably the most visual signs of life, which are even observable on Earth from outer space (Kräutler & Matile, 1999). Indeed, the temporal apparent 'recycling' of the green pigment Chl by seasonally alternating *de-novo* Chl biosynthesis and Chl degradation, on land and in the oceans, involves an estimated 1000 million tons, worldwide (Hendry, Houghton, & Brown, 1987; Morel, 2006). Strikingly, until about 30 years ago, Chl seemed to disappear in higher plants without leaving a trace, and non-green products of Chl breakdown remained elusive (Hendry et al., 1987; Matile, Ginsburg, Schellenberg, & Thomas, 1987). As we know today, the bilin-type Chl breakdown products, now generally named phyllobilins (PBs) (Kräutler, 2014), accumulate in higher plants as easily overlooked, colorless linear tetrapyrroles, primarily (Hörtensteiner, 2013; Hörtensteiner & Kräutler, 2011; Kräutler, 2016; Kräutler, Jaun, Bortlik, Schellenberg, & Matile, 1991; Kräutler & Matile, 1999; Kuai, Chen, & Hörtensteiner, 2018), the structures of which are related in a remarkable way to those of bilins, the products from heme breakdown (Falk, 1989).

First traces of presumed non-green Chl breakdown products were detected by Matile, Thomas and coworkers, when these authors compared the pigment pattern of senescent leaves of wild type *Festuca pratensis* with those in 'stay green' mutants of this grass (Matile, 1987; Thomas, Bortlik, Rentsch, Schellenberg, & Matile, 1989). Colorless compounds that were absent in the green mutant could be spotted in the wild type and were considered to represent some of the elusive Chl catabolites. They were called 'rusty pigments', as they rapidly converted into rust-colored products (Bortlik, Peisker, & Matile, 1990). One such 'rusty pigment' from senescent leaves of barley (*Hordeum vulgare*) could be isolated without degradation and color formation, and its structure was elucidated in 1991 with the help of modern spectroscopic means (Kräutler et al., 1992; Kräutler et al., 1991). It was confirmed to be a Chl catabolite, as it was a deconjugated bilin-type linear tetrapyrrole that carried the characteristic ring C/E-portion and other structural hallmarks of the Chls (Kräutler et al., 1991). This compound from barley was named the 'nonfluorescent' Chl catabolite (NCC) *Hv*-NCC-1 (**1**) (Scheme 1). The structure of NCC **1** indicated oxidative ring opening of the Chl macrocycle between C4 and C5 and **1** was first described as a 4,5-secophytoporphyrinoid (Kräutler et al., 1992; Kräutler et al., 1991). This 'northern' cleavage site contrasted with all expectations from Chl chemistry (Brown, Houghton, & Hendry, 1991), but turned out to be strikingly reminiscent of the site of ring opening in heme breakdown (Wilks, 2008). However, the meso-carbon C5 of

Chl *a* was retained in the formyl group of the NCC **1**, in contrast to the typical bilins from heme breakdown (Falk, 1989; Wilks, 2008), but similar to some heme-cleavage products observed in bacteria (Wilks & Ikeda-Saito, 2014). Additional polar groups at the molecular periphery of **1** pointed to puzzling catabolic processes in the formation of **1** from Chl, raising further questions with respect to the biochemistry of Chl breakdown in higher plants. As the NCC **1** was produced in barley leaves in experimental darkness, its key relevance for typical Chl breakdown in the fall leaves was not unambiguous.

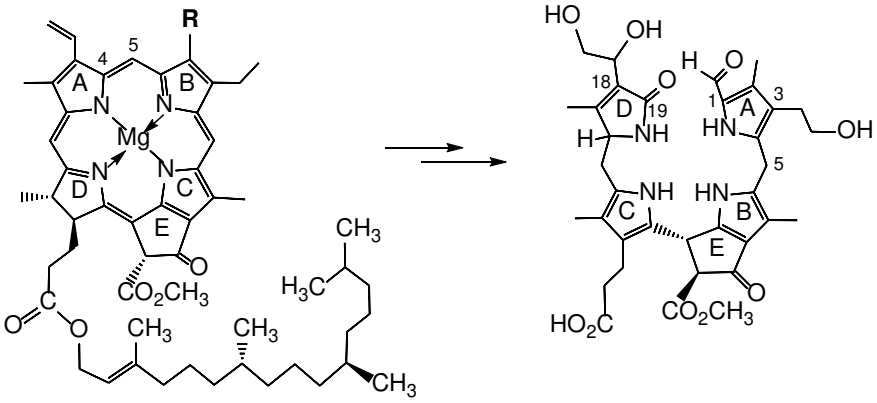

Scheme 1. Structural formulae of chlorophylls *a* and *b,* and of the first identified bilin-type Chl catabolite, the phyllobilane *Hv*-NCC-1 (**1**). Atom numbering of the two tetrapyrroles and labels of their 5-membered rings (A-E) follow the conventions for natural porphyrinoids (left) and bilins (right), differing systematically in the two types of compounds.

In the event, similar NCCs were soon found in naturally senescent leaves of the dicot oilseed rape (*Brassica napus*) (Mühlecker & Kräutler, 1996; Mühlecker, Kräutler, Ginsburg, & Matile, 1993). All of these NCCs carried a methyl group at their ring A, indicating their more direct lineage with Chl *a* (Kräutler, 2016). Much of the puzzle is now deciphered, how the NCCs are generated in the higher plants (Hörtensteiner & Kräutler, 2011), what happens to Chl *b* (Hörtensteiner, 2013; Kuai et al., 2018; Scheumann, Schoch, & Rüdiger, 1999; Tanaka & Tanaka, 2006; Tanaka, Kobayashi, & Masuda, 2011), and how the outset of senescence-induced Chl breakdown is subjected to interactive regulatory processes (Hörtensteiner, 2009; Tanaka & Tanaka, 2011). Pheophorbide *a* (Pheide *a*) has been identified as the ultimate intermediate with an intact porphyrinoid macrocycle (see Scheme 2 and later sections of this chapter) (Hörtensteiner, 2013). The specific oxygen-dependent cleavage of the macrocycle of Pheide *a* by Pheide *a* oxygenase (PAO) generates the 'red Chl catabolite' (RCC) (Kräutler, 2019; Kräutler, Mühlecker, Anderl, & Gerlach, 1997; Rodoni et al., 1997a), a cryptic red formyloxo-

bilin that represents the common precursor of the natural Chl-derived PBs in angiosperms (Hörtensteiner, Wüthrich, Matile, Ongania, & Kräutler, 1998; Pružinská, Anders, Tanner, Roca, & Hörtensteiner, 2003). Efficient enzymatic reduction (in a form of 'metabolic chanelling') of RCC by RCC reductases (RCCRs) (Rodoni, Vicentini, Schellenberg, Matile, & Hörtensteiner, 1997b; Sugishima, Kitamori, Noguchi, Kohchi, & Fukuyama, 2009; Wüthrich, Bovet, Hunziker, Donnison, & Hörtensteiner, 2000) next produces a first type of a fluorescent formyloxobilin (fluorescent type-I PB), the *'primary'* fluorescent Chl catabolites (*p*FCCs). Depending on the plant species, the blue fluorescent *p*FCCs is formed stereospecifically in one of two C16-epimeric versions, **2** or ***epi*-2** (Kräutler, 2016; Mühlecker, Kräutler, Moser, Matile, & Hörtensteiner, 2000; Mühlecker, Ongania, Kräutler, Matile, & Hörtensteiner, 1997). Typical '*modified'* FCCs (*m*FCCs) are produced from the two epimeric *p*FCCs by the action of chloroplastic or cytosolic enzymes (Hörtensteiner & Kräutler, 2011; Kuai et al., 2018). Most FCCs exist only fleetingly and isomerize spontaneously in the weakly acidic media of the vacuoles to the corresponding NCCs (Oberhuber, Berghold, Breuker, Hörtensteiner, & Kräutler, 2003; Oberhuber, Berghold, & Kräutler, 2008). Alternatively, *p*FCCs and 3^2-hydroxy-*p*FCCs (**3** and ***epi*-3**), are deformylated effectively by a cytochrome P450 mono-oxygenase (CYP) - identified in *Arabidopsis thaliana* (*Arabidopsis*) as CYP89A9 (Christ et al., 2013) – that furnishes corresponding dioxobilin-type fluorescent Chl catabolites (DFCCs), which isomerize rapidly and stereospecifically to natural dioxobilin-type NCCs (DNCCs) (Süssenbacher, Hörtensteiner, & Kräutler, 2015a). Indeed, two major lines of colorless, 'nonfluorescent' Chl catabolites (or phyllobilanes) are now known to accumulate in senescent leaves of angiosperms, representing NCCs ('nonfluorescent' type-I PBs) (Kräutler, 2014) or dioxobilin-type NCCs (DNCCs, 'nonfluorescent' type-II PBs) (Kräutler, 2016). As was the case for the first NCC to be discovered, the first DNCCs, then called 'urobilinogenoidic' Chl catabolites, also happened to be found in barley leaves (Losey & Engel, 2001).

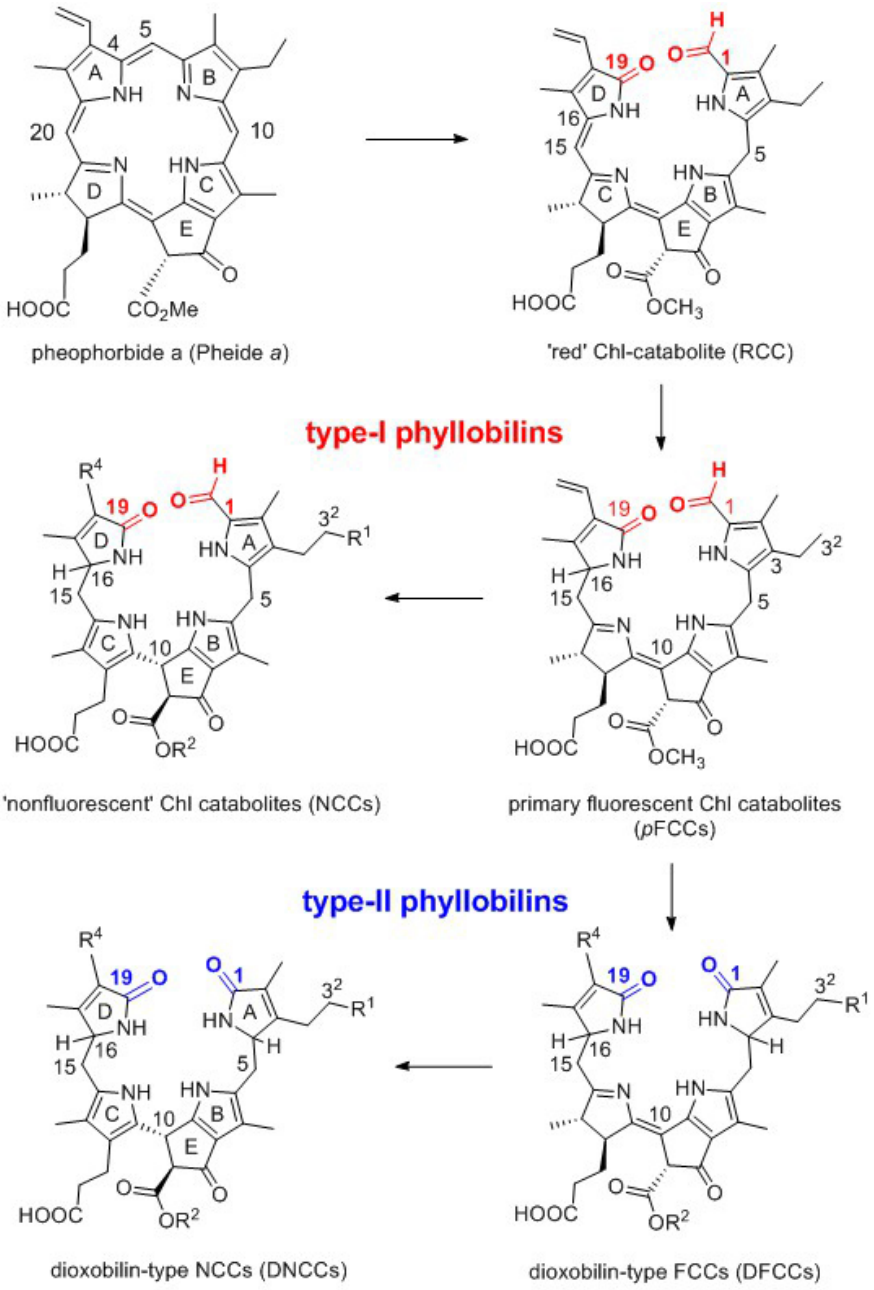

Scheme 2. Structural outline of central steps of Chl breakdown in higher plants. The 'red' Chl catabolite (RCC) is the common 1-formyl-19-oxobilin type precursor of all phyllobilins (PBs) along the PAO/phyllobilin pathway. The latter branches into two major lines at the stage of the colorless FCCs (fluorescent 1-formyl-19-oxobilin type PBs), which can undergo deformylation to fluorescent 1,19-dioxobilin type PBs (DFCCs). Both types of fluorescent PBs isomerize rapidly to corresponding 'nonfluorescent' 1-formyl-19-oxobilin type (NCCs) or 1,19-dioxobilin type PBs (DNCCs), representing type-I or type-II PBs, respectively.

II. Structures of Chl catabolites (phyllobilins) from higher plants and their nomenclature

A mostly phenomenological nomenclature was used in the earlier investigations on Chl catabolites (phyllobilins), which were named by the specification of the plant of origin, the basic structure type and a measure of polarity, e.g. as *Bn*-NCC-1 to *Bn*-NCC-3 for the three NCCs from oilseed rape (Mühlecker & Kräutler, 1996). Since then, several lines of practical phenomenological nomenclature have been developed in different laboratories (Christ, Hauenstein, & Hörtensteiner, 2016; Moser, Müller, Holzinger, Lutz, & Kräutler, 2012; Roca, Rios, & Perez-Galvez, 2018). In addition, a first structure-based semi-systematic nomenclature of Chl catabolites described them as 4,5-seco-phytoporphyrins (Kräutler et al., 1991; Kräutler & Matile, 1999). Following the introduction of the general naming of tetrapyrrolic Chl catabolites as 'phyllobilins' (PBs) (Kräutler, 2014), nomenclature rules from the bilin literature (Falk, 1989) are used, as also exemplified in this review. In line with this transition, atom renumbering was also adapted in 2014 (Kräutler, 2014). NCCs, such as **1** (Scheme 1), were more systematically classified on the basis of their structures as type-I phyllobilanes (Kräutler, 2014). Hence, **1** is named the 8^2S,10*R*,16*n*-3^2,18^1,18^2-trihydroxy-1-formyl-19-oxo-16,19-dihydrophyllobilane (Kräutler, 2014, 2016). This structure-based nomenclature clearly identifies PBs as specific compounds, independent of their origin from particular plants, and is used, nowadays, in parallel with the established phenomenological names, like *Hv*-NCC-1 (Christ et al., 2016; Kräutler, 2016; Moser et al., 2012; Roca et al., 2018). For practical reasons the chemical formulae of PBs are generally presented in a pseudocyclic form, in spite of the flexible nature of many of them and their presumed preference in more stable, extended structures (Kräutler, 2014). The crystal structure of an RCC-derivative (Engel, Gossauer, Gruber, & Kratky, 1993), of two yellow- (Li et al., 2018; Li et al., 2016) and of a pink-colored PB (Li et al., 2014), as well as some structures calculated by quantum chemical methods (Erhart et al., 2018a; Scherl et al., 2016), have helped to convey a more precise three-dimensional picture of selected PBs (Kräutler, 2016) (see below).

A. Colorless fluorescent phyllobilins from higher plants and their structures

1. Fluorescent (formyloxobilin-type) Chl catabolites

In the late 1980s colorless metabolites with a strong blue fluorescence, named FCs, were detected by Matile and coworkers in senescent leaves of barley, and were discussed in the context of Chl breakdown.(Düggelin, Schellenberg, Bortlik, & Matile, 1988) In a targeted preparative assay, using an active extract of senescent leaves of oilseed rape, the first fluorescent Chl catabolite (FCC) was obtained and identified as *p*FCC (**2**, 8^2S,10Z,12*S*,13*R*,16*n*-1-formyl-19-oxo-12,13,16,19-tetrahydro-phyllobilene-*b*) by detailed

structural characterization (Mühlecker et al., 1997). The phyllobilene-*b* **2** featured a structure that was key for assigning the hypothetical role of its direct precursor to the elusive RCC, a crucial cryptic intermediate of Chl breakdown (Mühlecker et al., 1997) along the common PAO/phyllobilin pathway (Hörtensteiner & Kräutler, 2011) (Scheme 2). In a related study with senescent leaves of sweet pepper (*Capsicum annum*), its main FCC was characterized as the C16-epimer of **2**, called *epi-p*FCC (***epi*-2**) (Mühlecker et al., 2000). Hence, the *p*FCCs are produced in one of two C16-epimeric forms by the stereospecific reduction of the C15=C16 double bond of RCC by one of two lines of cofactor-free RCCRs, establishing the deep rooted relevance of two stereo-types of RCCRs (Hörtensteiner et al., 2000). An electrochemical reduction process modeled a stereounspecific version of RCC reduction by the RCCRs (Kräutler, 2019; Oberhuber et al., 2008). Typical FCCs, now also classified as fluorescent type-I PBs (Kräutler, 2016), do not accumulate in plant cells and disappear quickly, either by rapid isomerization to corresponding NCCs (in the weakly acidic medium of the vacuoles, in particular) (Christ et al., 2012; Oberhuber et al., 2003; Oberhuber et al., 2008), or by deformylation to corresponding DFCCs on the way to type-II PBs (Christ et al., 2013; Hörtensteiner & Kräutler, 2011). For such reasons, the number of FCCs detected and characterized in studies of senescent leaves and ripening fruit is still inferior to the ones of the generally accumulating NCCs and DNCCs (Christ et al., 2016; Kräutler, 2016; Roca et al., 2018). Only a handful of *m*FCCs have been isolated from plant extracts and characterized structurally, such as *Mc*-FCC-62 (***epi*-3**, 3^2-hydroxy-*epi*-*p*FCC) (Moser et al., 2012), *At*-FCC-1 (**4**, 3^2-hydroxy-8^4-desmethyl-*p*FCC) and *At*-FCC-2 (**5**, 8^4-desmethyl-*p*FCC) (Pružinská et al., 2005) (see Table 1). UV/Vis-specta of FCCs display two closely spaced maxima, one around 360 nm (due to the conjugated system of rings B and C of FCCs), and a second absorption maximum around 320 nm, which is due to the characteristic α-formylpyrrole unit (ring A) of type-I PBs. The nearly colorless FCCs show a strong blue fluorescence with an emission maximum near 450 nm and photoexcited FCCs sensitize the formation of singlet oxygen very effectively (Jockusch, Turro, Banala, & Kräutler, 2014).

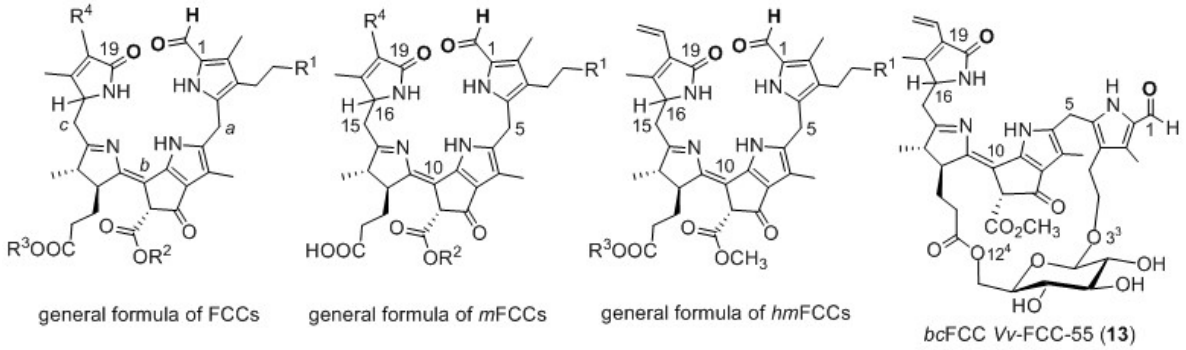

Scheme 3. General formula of FCCs, *m*FCCs, and of *hm*FCCs, and formula of the *bc*FCC *Vv*-FCC-55 (**13**) (see Table 1). FCCs constitute the PB-class of the type-I phyllobilenes-*b*.

In ripe, yellow bananas (*Musa acuminata* cv. Cavendish) first persistent FCCs were detected in 2008, as well as the strong blue fluorescence of ripe bananas was discovered, which is easily seen, when observed under 'black (UV)-light' (Moser et al., 2008a). This new type of exceptionally persistent FCCs was revealed to carry an unprecendented sugar-containing ester function at their propionate side chain (Scheme 3 and Table 1). They were classified as 'hypermodified' FCCs (*hm*FCCs), such as the banana FCCs *Mc*-FCC-56 (**6**), *Mc*-FCC-53 (***iso*-6**), *Mc*-FCC-49 (**7**) and M*c*-FCC-46 (***iso*-7**) (Moser et al., 2008a; Moser et al., 2009). Similar persistent *hm*FCCs were also detected as the natural FCCs *Ma*-FCC-61 (**8**) (Banala et al., 2010), *Ma*-FCC-64 (**9a**) (Vergeiner, Banala, & Kräutler, 2013) and *Ma*-FCC-63 (**9b**) (Vergeiner et al., 2013), and *Sw*-FCC-62 (**10**) (Kräutler et al., 2010), respectively, in extracts of senescent leaves of banana plants (*Musa acuminate*) or of peace lily (*Spathiphyllum wallisii*). However, the likewise identified persitent methyl ester **11** of ***epi*-3** was classified as an isolation artefact in the methanolic banana peel extract (Moser et al., 2012). Interestingly, some of the *hm*FCCs from bananas carried an additional β-glucopyranosyl unit appended to their 3^2-hydroxygroup, such as *Mc*-FCC-49 (**7**) and *Mc*-FCC-46 (***iso*-7**) (Moser et al., 2009; Moser et al., 2012). Such sugar appendages have frequently been observed at $C3^2$ in the more abundant NCCs, (Kräutler, 2016) and a corresponding 3^2-β-glucopyranosylated *m*FCC (3^2- β -glucopyranosyl-*p*FCC **12**) has also tentatively been identified in *Arabidopsis* (Christ et al., 2012). Remarkably, all of the known *hm*FCCs still carry at their ring D a vinyl group and a methyl ester group at $C8^2$ of ring E, as are present in the Chls (see Table 1).

Table 1 here

A unique combination of the substituent pattern of *hm*FCCs and of 3^2-glycopyranosyl FCCs was discovered in senescent leaves of grapevine (*Vitis vinifera*, cv. Chardonnay), where the *Vv*-FCC-55 (**13**) was characterized, a so called bicyclo[17.3.1]-1',6'-glycopyranosyl-FCC ('bicyclo'-FCC, *bc*FCC), in which a β -glucopyranosyl unit is attached twice, once - glycosidic - at $O3^2$, and once - as an O6' glucosyl-ester moiety at the propionate substituent (see Scheme 3) (Erhart et al., 2018a). The bicyclo[17.3.1]-1',6'-glycopyranosyl moiety imposes a fairly rigid three dimensional structure upon *Vv*-FCC-55 (**13**), a remarkably stable, novel type of a *hm*FCC (Erhart et al., 2018a), conspicuously related to *Vv*-DFCC-53 (**14**) the fluorescent type-II analog

(see below).

2. Dioxobilin-type fluorescent Chl catabolites

The first dioxobilin-type FCCs (DFCCs) were identified in (wild type) *Arabidopsis* (Christ et al., 2013; Süssenbacher et al., 2015a). Typical DFCCs or fluorescent type-II PBs were assigned the role of the direct precursors of the more abundant DNCCs (Christ et al., 2013; Kräutler, 2016). The polar and short lived *At*-DFCC-33 (**15**), with 'n'-configuration at C16, but unknown at C4, named 8^2*S*,10Z,12*S*,13*R*,16*n*-1,19-dioxo-1,4,12,13,16,19-hexahydro-phyllobilene-*b*, was observed to isomerize stereospecifically and rapidly to a corresponding DNCC, named *At*-DNCC-33 (**16**) (Süssenbacher et al., 2015a). Likewise, in the *mes16* mutant of *Arabidopsis* (see below), the astoundingly hydroxymethylated *At*-2HM-*iso*-DFCC (**17**) was identified and characterized (Scheme 4) (Süssenbacher, Christ, Hörtensteiner, & Kräutler, 2014), which appears to be the direct metabolic precursor of the corresponding *At*-2HM-*iso*-DNCC (**18**) (see below) (Süssenbacher et al., 2014). UV/Vis-specta of DFCCs display a maximum around 360 nm, like FCCs, but lack the second absorption maximum of the type-I PBs, at around 320 nm, which is due to their α-formylpyrrole unit. However, photoexcited DFCC **15** shows a similarly strong blue emission as FCCs (Süssenbacher et al., 2015a).

In senescent grapevine leaves the unique DFCC **14** was detected, an analog of the bicycloglycosidic *Vv*-FCC-55 (**13**). It was characterized structurally as a bicyclo[17.3.1]-1',6'-glycopyranosyl-DFCC (a *bc*DFCC) (Scheme 4) (Erhart et al., 2018a), assigning **14** the role of the formal direct product of the oxidative deformylation of the *bc*FCC **13**. Interestingly, in the *bc*DFCC **14** the absolute configuration of the newly introduced stereocenter at C4 could indirectly be deduced as *R* from NMR-studies in combination with model structures from high level theoretical calculations (Erhart et al., 2018a). However, the biochemistry of the metabolic formation of such extraordinary bicyclo[17.3.1]-1',6'-glycopyranosyl-PBs still is abscure, as are the enzymes catalyzing attachment of the bicyclo[17.3.1]-1',6'-glycopyranosyl moiety to the bilin-type tetrapyrrole core.

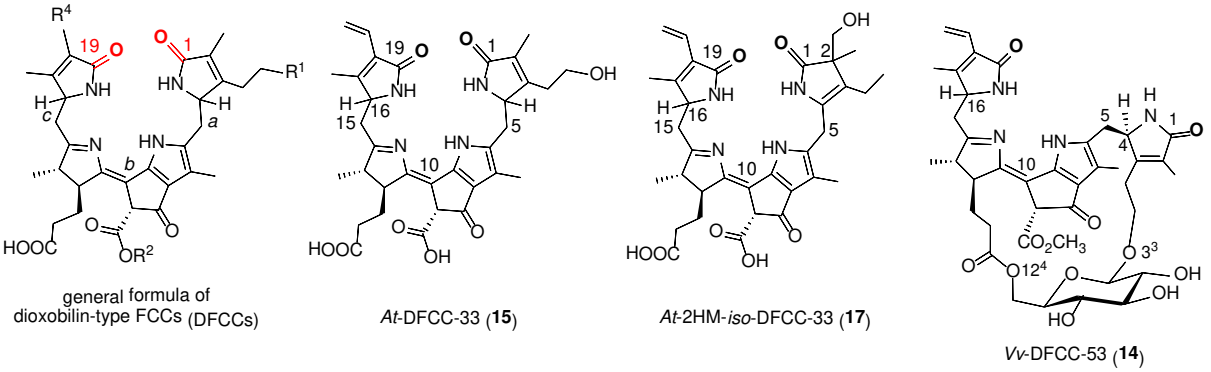

Scheme 4. General formula of DFCCs and formula (left to right) of *At*-DFCC-33 (**15**), of the *iso*-DFCC *At*-2HM-*iso*-DFCC (**17**), and of the *bc*DFCC *Vv*-DFCC-53 (**14**). DFCCs constitute the class of the type-II phyllobilenes-*b*.

B. Colorless nonfluorescent phyllobilins from higher plants and their structures.

The so called 'nonfluorescent' Chl catabolites (NCCs), now classified alternatively as formyloxobilin-type phyllobilanes (or as type-I phyllobilanes) (Kräutler, 2016) are the most numerous group among the known natural Chl catabolites (see Table 2). The colorless NCCs accumulate in senescent leaves, and one of them also happens to represent the first bilin-type Chl catabolite to be characterized (Kräutler et al., 1991).

1. Formyloxobilin-type nonfluorescent Chl catabolites

Over 20 structurally different natural NCCs have been identified, so far, in senescent leaves (Christ et al., 2016; Curty & Engel, 1996; Kräutler, 2016; Kräutler et al., 1991; Mittelberger et al., 2017; Roca et al., 2018), vegetables (Berghold, Breuker, Oberhuber, Hörtensteiner, & Kräutler, 2002; Roiser, Müller, & Kräutler, 2015) and fruit (Moser et al., 2012; Müller, Ulrich, Ongania, & Kräutler, 2007; Rios, Perez-Galvez, & Roca, 2014a; Rios, Roca, & Perez-Galvez, 2014b; Roca, Rios, Chahuaris, & Perez-Galvez, 2017; Vergara-Dominguez, Rios, Gandul-Rojas, & Roca, 2016) (see Table 2). Many of these could be isolated and their actual chemical structures were determined (Kräutler, 2016). The natural NCCs all show not only a common tetrapyrrolic core but feature, in addition, a common stereochemistry at their meso C10 position. However, there are two C16 epimeric lines of NCCs, just as with their FCC precursors. It has been proposed (Oberhuber et al., 2003) and is generally agreed today that typical natural NCCs are formed directly from their corresponding FCC precursors by a remarkable non-enzymatic isomerization that is acid-activated and is presumed to take place in the vacuole, predominantly (Kuai et al., 2018; Oberhuber et al., 2003). This stereospecific chemical process transforms the apparently less stable FCCs, or type-I phyllobilenes-*b*, into the more stable NCCs, where ring C is a third aromatic pyrrole ring (Kräutler, 2016, 2019). The isomerization deconjugates the namegiving fluorophore of the blue luminescent FCCs into a non-luminescent dipyrromethane unit (see Scheme 5). At the same time it establishes the configuration at the new asymmetric center C10, which has *R*-configuration in the known type-I phyllobilanes (Kräutler, 2016). The adjacent asymmetric $C8^2$ has *S*-configuration in the predominant forms of the NCCs. However, $C8^2$ is part of a β-ketoester grouping at ring E, which promotes slow equilibration of the main isomer with the minor, $C8^2$-*R*-epimer (Moser, Scherzer, & Kräutler, 2017).

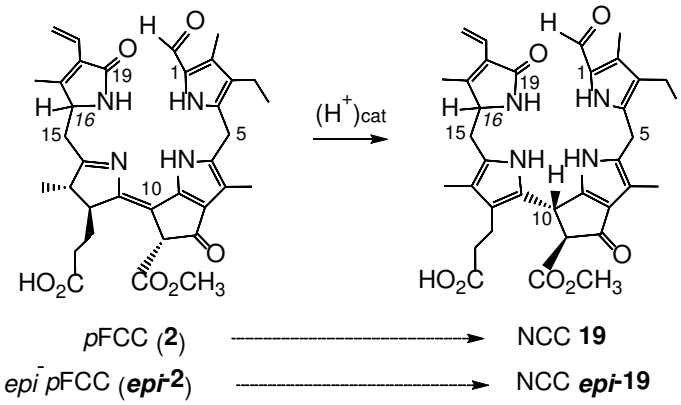

Scheme 5 The typical natural NCCs are generated by a non-enzymatic isomerization of FCCs that carry the free propionic acid substituent derived from Pheide *a* and RCC (Kräutler, 2016). In this process, *p*FCC (**2**) isomerizes to the NCC **19** (retaining C16-'n' configuration), and *epi*-*p*FCC (***epi*-2**) to the corresponding C16-epimer ***epi*-19** (retaining C16-'epi' configuration).

In most natural NCCs the propionic acid group is available as the free acid (R^3 = H; Scheme 6). In a few relatively apolar NCCs the 3-position is decorated with an ethyl group (R^1 = H). Much more common are more polar NCCs with R^1 at $C3^2$ represented by a hydroxygroup (such as in **1**) or with a β-glycopyranosyl or malonyl group attached to it (such as in *Bn*-NCC-2, **20** or *Bn*-NCC-1, **35**) (Mühlecker & Kräutler, 1996). At ring E the substituent may be a methyl ester function (as in **1**, directly derived from the Chls) or it is hydrolyzed to a free carboxylic acid group, such as in the NCCs from oilseed rape, such as **20** and **35**. The β-keto-carboxylate groups in the latter are surprisingly resistant against loss as carbon dioxide (Mühlecker & Kräutler, 1996), and the preparation of corresponding (decarboxylated) pyro-NCCs (*py*NCCs, such as **21**), by partial synthesis, required rather harsh synthetic conditions (Li et al., 2018). Surprisingly, genuine natural *py*NCCs are not known (Li et al., 2018). The substituent R^4 at ring D often is a vinyl group, a stereouniform 1,2-dihydroxy-ethyl group (as in **1**), or an 18^1-hydroxy,18^2-β-glycopyranosyl-ethyl group, as discovered in the 3^2,18^2-diglycosylated type-I phyllobilane *Pd*-NCC-32 (**22**) from plum (*Prunus x domestica*) (Erhart et al., 2016). *Mc*-NCC-58 (**23**) and *Mc*-NCC-55 (**24**), two minor NCCs in extracts of the outer peels of ripe bananas [*Mc*-NCC-58 (**23**) and *Mc*-NCC-55 (**24**)] were provisionally identified as isomers of the main *hm*FCC from this source, hence, tentatively characterized as NCCs carrying a daucic acid ester function at their propionic acid side chain (Moser et al., 2012). A first bicyclo[17.3.1]-1',6'-glycopyranosyl-NCC [the *bc*NCC *Ug*-NCC-53 (**25**)] was identified in extracts of wych elm (*Ulmus glabra*) leaves, an exceptional type-I phyllobilane, in which a 1',6'-glycopyranosyl-linker bridges the phyllobilane skeleteton at $O3^3$ (at ring A) and $O12^4$ (at ring C) (Scherl, Müller, & Kräutler, 2012) (see Scheme 6). Stable NCCs from a variety of different plant species

may have identical structures, such as ***epi*-26** (*Cj*-NCC-1, discovered in *Cercidiphyllum japonicum*)(Curty & Engel, 1996), but also identified in other plants, as e.g., *So*-NCC-4, *Pc*-NCC-2, *Md*-NCC-2, *Mc*-NCC-61, *Ej*-NCC-4 (Kräutler, 2016; Roca et al., 2018). In other cases, NCCs differ characteristically by their configuration at C16, i.e, they may be pairwise C16-epimers, such as the isomeric NCCs ***epi*-26** (*Cj*-NCC-1) and **26** (detected as *Sw*-NCC-58 in senescent leaves of the peace lily) (see Table 2).

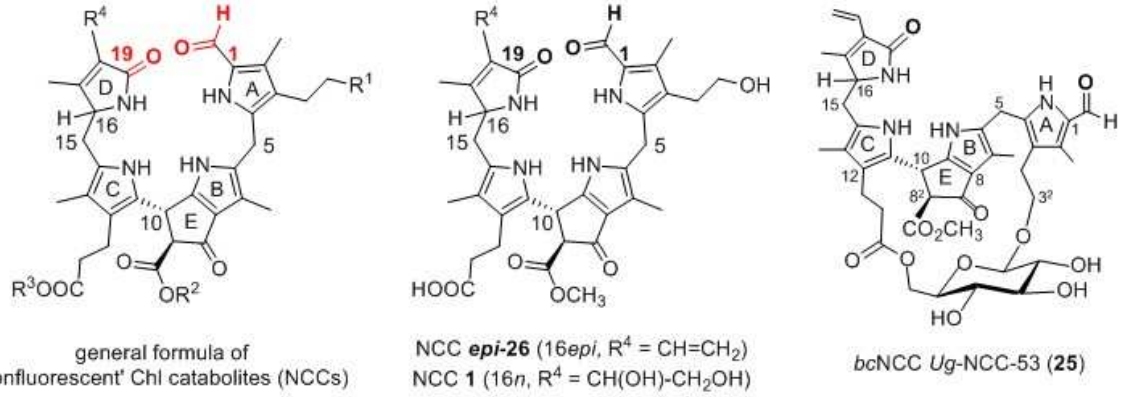

Scheme 6. General formula of NCCs and formulae of the typical natural NCCs **1**, ***epi*-26**, and of the *bc*NCC *Ug*-NCC-53 (**25**) (see Table 2). NCCs constitute the class of the type-I phyllobilanes.

Table 2 here

2. Dioxobilin-type nonfluorescent Chl catabolites (DNCCs)

In senescent leaves of barley two isomeric forms of dioxobilin-type NCCs (DNCCs) were first described by Losey and Engel, which classified the two type-II phyllobilanes **37** and **38** as 'urogenobilinoidic' Chl catabolites. This finding was considered a first sign of a further oxidative deformylation of the NCC **1** (Scheme 7) (Losey & Engel, 2001). Strikingly, in senescent leaves of Norway maple no NCCs were detected, but the *Ap*-DNCC **39**, a further stereo-isomer of the two 'urogenobilinoidic' *Hv*-DNCCs (Müller, Rafelsberger, Vergeiner, & Kräutler, 2011). The (pseudo-) mirror image relationship of **39** (from CD-spectra) with the two DNCCs from barley was considered remarkably incompatible with an NCC precursor, and suggested the involvement of unknown transformations of Chl catabolites that would occur earlier on the PAO/phyllobilin pathway, e.g., at the stage of a properly structured FCC (Müller et al., 2011). Indeed, as is described in more detail below, the massive accumulation of a range of DNCCs in senescent leaves of *Arabidopsis* could soon be rationalized by the activity of a CYP that deformylated some FCCs very effectively (Christ et al., 2013).

In the meantime, a variety of DNCCs have been described from various plant sources (see Table 3), including senescent leaves (Christ et al., 2016; Kräutler, 2016; Losey & Engel, 2001; Roca et al., 2018), vegetables (Roiser et al., 2015) and fruits (Rios et al., 2014a; Roca et al., 2018), establishing, together with their presumed fluorescent precursors (DFCCs), the 'second' line of the dioxobilin-type PBs, now all also classified as type-II PBs (Kräutler, 2014, 2016; Kuai et al., 2018). Interestingly, an intimate structural and chemical relationship between the DFCC *At*-DFCC-33 (**15**) and the main DNCC, *At*-DNCC-33 (**16**) of *Arabidopsis* could be established in the chemical isomerization of **15** to **16**. This indicated the same type of stereochemical correlation and non-enzymatic mechanism of DNCC formation (Süssenbacher et al., 2015a), as first deduced for the relationship between FCCs and NCCs (Oberhuber et al., 2003). Accordingly, in further agreement with the chiroptical properties of the presently known natural NCCs and DNCCs (with the exception of *Ap*-DNCC **39**), the stereochemistry at C10 is tentatively deduced to be the same, i.e. to display *R*-configuration (Kräutler, 2016; Süssenbacher et al., 2015a). In the case of the *bc*DFCC *Vv*-DFCC-53 (**14**) from senescent leaves of grape vine, the new asymmetric C4 at ring A of this type-II PB was also deduced to have *R*-configuration (see Scheme 4). The relevance of the tentative stereochemical assignement *R* of C4 in *Vv*-DNCC-51 (**40**) from the same plant (Erhart et al., 2018a) remains to be established, as is the configuration of C4 of other DFCCs and DNCCs. The stereochemistry of this methine carbon is an indirect result of the oxidative deformylation by a CYP enzyme (CYP89A9 in *Arabidopsis*) (Christ et al., 2013), which may exhibit different signs and degrees of stereoselectivity in different angiosperms.

In *Arabidopsis* type-II PBs with a strikingly altered ring A structure have been observed as results of (an apparently aberrant) metabolism of *p*FCC (**2**) molecules that escape hydroxylation by TICC55. This catabolic line produces dioxobilin-type phyllobilanes that carry an additional hydroxymethyl group at C4 of their ring A, such as *At*-4HM-DNCC-41 (**41**) and At_{mes16}-4HM-DNCC-44 (**42**), or in their regio-isomers *At*-2HM-*iso*-DNCC-43 (**43**) and At_{mes16}-2HM-*iso*-DNCC-46 (**44**) (see Scheme 7). These nonfluorescent DCCs (NDCCs) are presumed to be isomers and descendants of the correspondingly altered fluorescent DCCs, such as *At*-2HM-*iso*-DFCC (**16**) (Süssenbacher, Kreutz, Christ, Hörtensteiner, & Kräutler, 2015b).

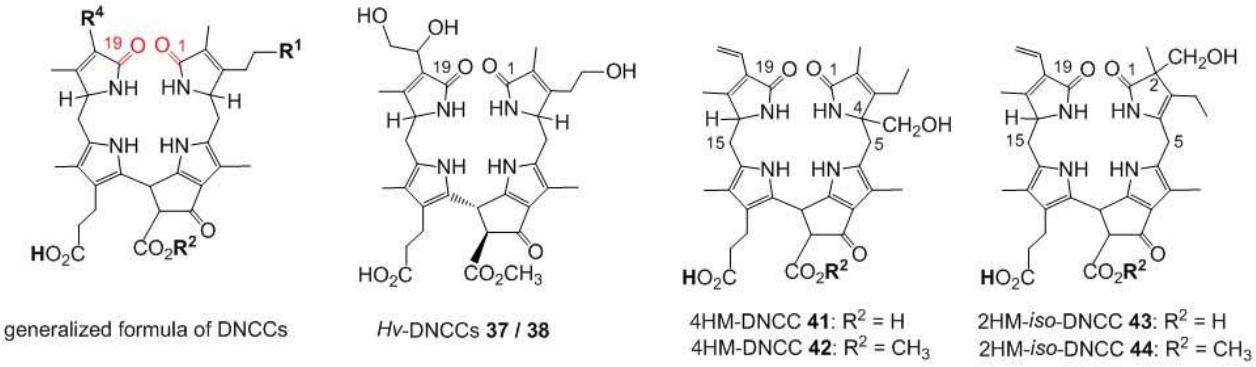

Scheme 7. General formula of dioxobilin-type NCCs (DNCCs), and formulae of (left to right) *Hv*-DNCCs **37** and **38**, the 4HM-DNCCs **41** and **42**, and the 2HM-*iso*-DNCCs **43** and **44**. DNCCs constitute the class of the type-II phyllobilanes.

Table 3 here

3. Isophyllobilanones

So far, studies of Chl breakdown in higher plants, as well as of their bilin-type Chl catabolites (Kräutler, 2016), have nearly exclusively dealt with angiosperms (Hörtensteiner & Kräutler, 2011; Kuai et al., 2018; Tanaka et al., 2011). Very recently have Chl catabolites in the extracts of senescent leaves of bracken (*Pteridium aquilinum*) been investigated, i.e. from a member of the large plant division of the ferns (Erhart, Vergeiner, Kreutz, Kräutler, & Müller, 2018b). The structures of two of the tetrapyrrolic catabolites turned out to differ remarkably from the so far identified PBs. Their structures displayed an unprecendented (C6 to C7)-rearranged carbon skeleton. Furthermore, the new structures reflected the basic elements of a *py*NCC, lacking a substituent at $C8^2$ of ring E, and unprecedented with natural PBs (Li et al., 2018). In addition, an extra oxygen atom decorated their ring B moiety in a novel vinylogous imide functionality (see Scheme 8). Therefore the two fern Chl catabolites were classified as isophyllobilanones (*i*PBons) (Erhart et al., 2018b). However, the structures of both of the *i*PBons (**47**,**48**) relate to the formyloxobilin pattern known in type-I PBs from angiosperm. This indicates the key activity, in the fern, of enzmes that are related to PAO and cleave the porphyrinoid macroring oxygenolytically at the northern meso-position (Hörtensteiner et al., 1998). Furthermore, a peripheral hydroxylation at $C3^2$ reminds of the activity of the hydroxylase TIC55 (translocon at the inner chloroplast membrane 55) (Hauenstein, Christ, Das, Aubry, & Hörtensteiner, 2016), and a chromophore reduction analogous to the one of the known RCCRs (Rodoni et al., 1997b) appears to saturate C15 and C16 at the 'western' meso-position. The lack of a substituent at $C8^2$ of the *i*PBons suggests a more direct relationship with pyro-

Pheide (*py*Pheide) *a* (Scheer, 2006) than with Pheide *a* itself, a finding reminiscent of the structures of some red Chl catabolites, isolated from the green alga *Auxenochlorella protothecoides* (Engel, Curty, & Gossauer, 1996).

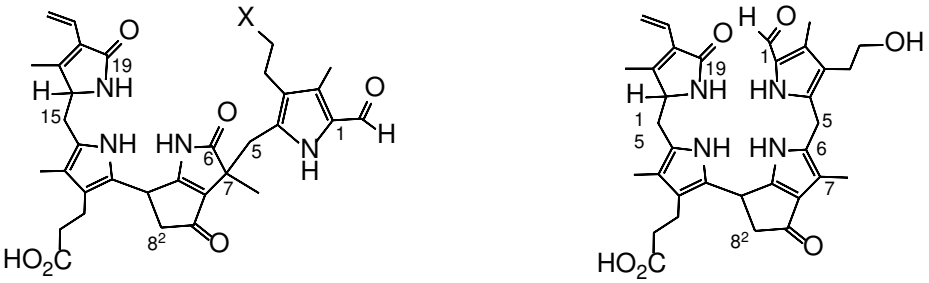

Scheme 8. Formulae of isophyllobilanones (*i*PBons) **47** and **48** from braken fern, and of the semisynthetic pyro-NCC (*py*NCC) **21**.

C. Phyllochromobilins - Colored phyllobilins in leaves and fruit

Consistent with the original name of the colorless NCCs as 'rusty pigments', NCCs typically undergo a ready transformation upon storage with exposure to air, when also exposed to day light, in particular, furnishing yellow-colored Chl catabolites (YCCs), first, and subsequently pink-colored Chl catabolites (PiCCs) (Ulrich, Moser, Müller, & Kräutler, 2011). The 'spontaneous' formation of such colored PBs (collectively named phyllochromobilins) is the visual sign of the extension of π-conjugated chromophores as result of an oxidation, which has been related to the antioxidant properties of NCCs and YCCs. First, the meso-position C15 is unsaturated, giving YCCs (Moser, Ulrich, Müller, & Kräutler, 2008b), which are subsequently oxidized further at C10, to furnish pink-colored PiCCs (Ulrich et al., 2011). In these colored PBs new intensive absorption bands near 430 nm and near 520 nm, respectively, are responsible for the bright colors of YCCs and PiCCs (Kräutler, 2016; Li et al., 2014).

1. Yellow phyllobilins

In some senescent leaves, where PBs typically accumulate as colorless linear tetrapyrroles, yellow (formyloxobilin-type) Chl catabolites (YCCs), also classified as type-I phylloxanthobilins (PxBs) have been detected as a new type of yellow plant pigments (Moser et al., 2008b) (see Scheme 9). Natural YCCs were first isolated from senescent leaves of *C. japonicum*, such as the one then named *Cj*-YCC-2 (**50**). YCCs are induced by day light to interconvert photoreversibly with their sligthly more polar isomer, such as **50** with **51**. The YCCs **50** and **51** were identified by NMR-spectroscopy as 15*Z*- and 15*E*-double bond isomers

(Moser et al., 2008b). The structures of the methyl esters (**Me-50** and **Me-52**) of the natural YCC **50** (Li et al., 2016) and of the related semisynthetic *pyro*-YCC **52** (Li et al., 2018), respectively, have been analysed by crystallography, confirming the solution structures, derived earlier, and revealing the formation of unique homochiral π-staked and H-bonded dimers (Li et al., 2016). More polar PxBs related to **50**, such as the YCCs **53** (Scherl et al., 2012) and **54** (Wakana et al., 2014) have also been detected in extracts of some senescent leaves (Kräutler, 2016; Scherl et al., 2012; Wakana et al., 2014) and ripening fruit (Roca et al., 2017) The YCC **50** is the indirect product of an endogenous oxidation, either of the NCC ***epi*-26** or of the epimeric NCC **26** (Vergeiner et al., 2015). A still puzzling regiospecific reaction oxidizes NCCs at their C15 to furnish polar analogues, which, by acid-induced elimination, convert easily and highly selectively into the 15Z-isomers of corresponding YCCs, such as **50** (Vergeiner et al., 2015) (Scheme 9 and Table 4).

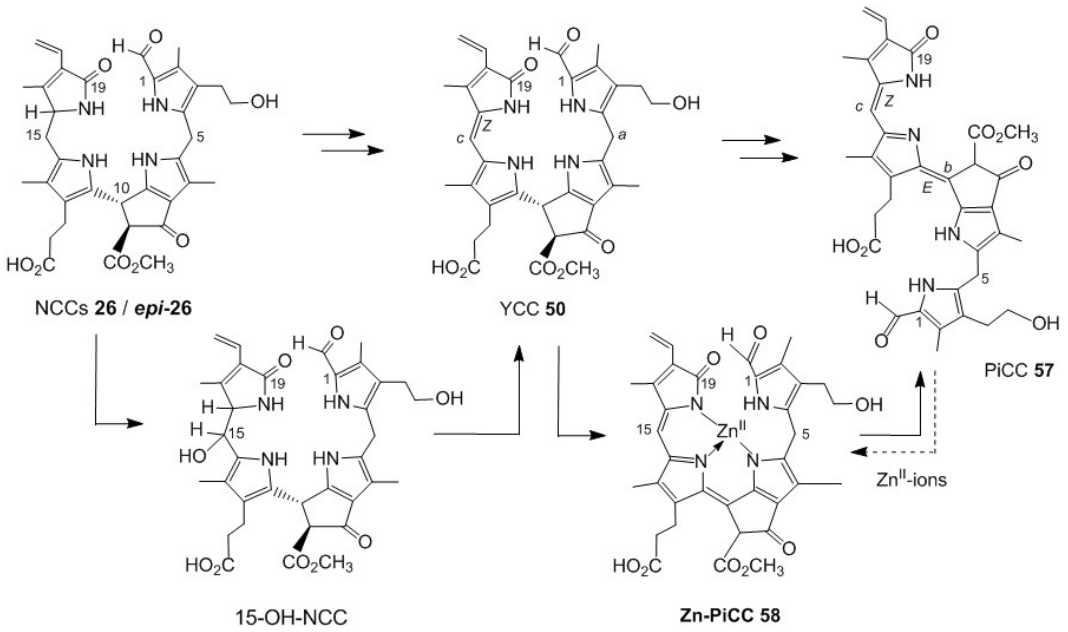

Scheme 9. Left. Formation of YCC **50** by oxidation of the C16-epimeric NCCs **26** and ***epi*-26** to corresponding intermediate 15-hydoxyl-NCCs. Right. Synthesis of PiCC **57** from YCC **50** *via* the Zn-complex Zn-PiCC **58**. YCCs are type-I PxBs or type-I phyllobilenes-*c*, PiCCs are type-I phyllobiladienes-*b,c*.

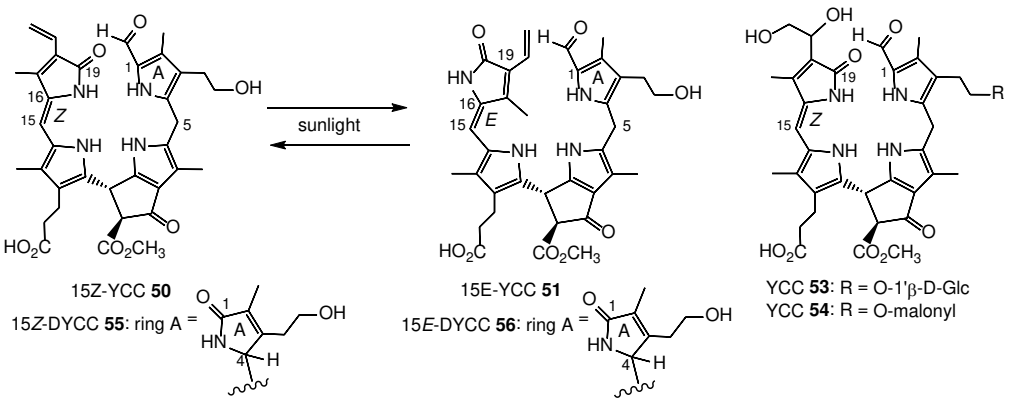

Scheme 10. Top. Formulae of the 15*Z*- and 15*E*-isomeric YCC-forms **50** and **51**, representing two natural YCCs, of the corresponding DYCCs **55** and **56**, and of the polar YCCs **53** and **54**. DYCCs constitute the class of the type-II phyllobilenes-*c*.

More recently, yellow Chl catabolites that lacked the absorption band near 320 nm (that is due to the α-formylpyrrole unit in type-I PBs) were detected in extracts of senescent leaves of grapevine (Erhart et al., 2018a) and of *Arabidopsis* (I. Süssenbacher, D. Menghini, S. Hörtensteiner and B. Kräutler, unpublished). They were provisionally described as dioxobilin-type yellow Chl catabolites (DYCCs or type-II PxBs). Similar to the mechanism of formation of YCCs from NCCs (Moser et al., 2008b), the pathway of the endogenous formation of DYCCs (yellow type-II PxBs) was proposed to involve oxidation of DNCCs. This was verified by the partial "green" synthesis of the DYCC **55** from the main grapevine leaf DNCC, *Vv*-DNCC-51 (**40**), using an extract of *S. wallisii* leaves in an aerated solution (Li, Erhart, Liu, & Kräutler, 2019). The synthetic DYCC was identified with the DYCC detected in extracts of senescent grapevine leaves (Li et al., 2019). Upon photoexcitation, the DYCC **55** (15Z form) underwent photoreversible 15*Z*/15*E* double bond isomerization to the less stable 15*E*-isomer **56**, as had been observed with YCCs (see Scheme 10). The yellow Chl catabolites, either of type-I or of type-II, carry a chromophore, first seen in bilirubin (Falk, 1989), and they also exhibit related (photo)chemistry.

2. Pink phyllobilins

The chromophore of yellow Chl catabolites, i.e. PxBs, lends itself for oxidation, causing extension of the conjugated π-system to rings B and E in PiCCs, or type-I phylloroseobilins (PrBs, see Scheme 11). Oxidation of aerated solutions of type-I PxBs leads to type-I PrBs (Kräutler, 2016), first described as the formyloxoblin-type PiCC **57** (Ulrich et al., 2011). The structure of this pink-colored type-I 10*E*,15*Z*-phyllobiladiene-*b*,*c*, first deduced from NMR-data, was confirmed by X-ray crystallography (Li et al., 2014).

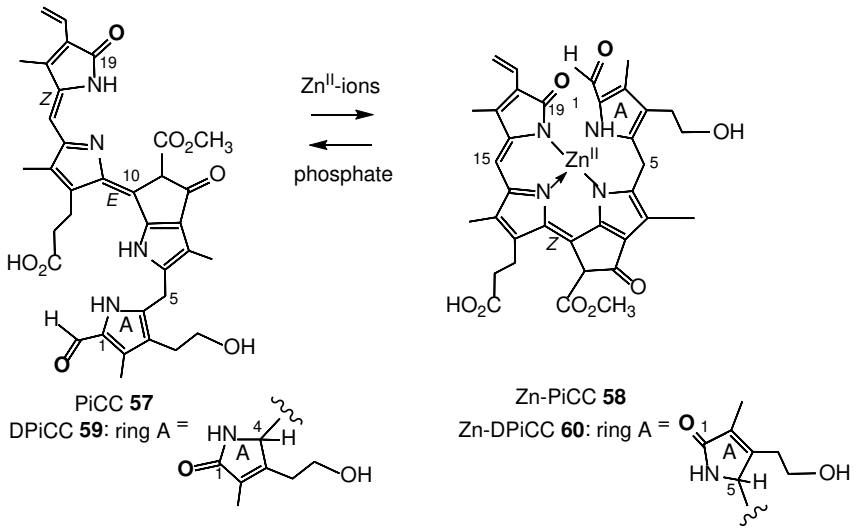

Scheme 11. The pink-colored PBs, PiCC **57** and DPiCC **59**, represent 10*E*,15*Z*-phyllobiladienes-*b*,*c* . Both, PiCC **57** and DPiCC **59**, bound Zn^{II}-ions remarkably well in a tridentate fashion, giving the blue Zn^{II}-complexes **58** and **60**, in which a 10Z,15Z-phyllobiladien-*b*,*c* represented the ligand (Li et al., 2014).

PiCC **57** binds transition metal ions remarkably well in a tridentate fashion, so that in the resulting blue metal complexes the ligand is present in a 10Z,15Z-phyllobiladien-*b*,*c* arrangement (Li et al., 2014). Transition metal binding induces a bathochromic shift of the long wavelength absorption maximum by about 100 nm from about 520 nm, in the practically non-luminescent PiCC (**57**) to about 620 nm, in the strongly red-fluorescent Zn-PiCC complex (**58**). Binding of a variety of divalent first and second row transition metal ions occurs rather tightly down to sub-nmol concentrations, and the YCC converted into the Zn-complex **58** directly and efficiently in an aerated methanolic solution at room temperature (Li et al., 2014). The Zn-ion can be removed by treatment with phosphate, so that the sequence YCC **50** to Zn-PiCC **58** to PiCC **57** is an efficient synthetic route to PiCCs (Li et al., 2014).

Similar experiments as those with the PiCC **57** and its Zn-complex **58** have been performed lately with the semisynthetic DYCC **55** that lacked the absorption band near 320 nm (of the α-formylpyrrole unit of type-I PBs). As described for the preparation of PiCCs from YCCs (Li et al., 2014), the oxidation of aerated solutions of the type-II PxB **55** led to the first dioxobilin-type pink Chl catabolite (DPiCC), the type-II PrB **59**. The structure of the PrB **59** was again deduced from NMR-data to represent a 10*E*,15*Z*-phyllobiladiene-*b,c* (Li & Kräutler, 2019). The DPiCC bound zinc ions remarkably well in a tridentate fashion, similarly as observed with the PiCC, giving blue metal complexes in which the ligand was present in a 10*Z*,15*Z*-phyllobiladiene-*b,c* arrangement (C. J. Li and B. Kräutler, unpublished). As seen with the PiCC

57, zink ion binding caused a large bathochromic shift of the long wavelength absorption maximum from 522 nm for the practically non-luminescent DPiCC **59**, to about 619 nm for the strongly red fluorescent Zn-DPiCC complex **60** (C. J. Li and B. Kräutler, unpublished). As found with the related type-I phyllochromobilins originally (Li et al., 2014), the DYCC **40** converted into the Zn-complex **60** directly in an aerated methanolic solution at room temperature, and the bound Zn-ion of the complex **60** could be removed by treatment with phosphate. Hence, the sequence DYCC **40** to Zn-DPiCC **60** to DPiCC **59** turned out to be an efficient semisynthetic route to the DPiCC **59** (Li & Kräutler, 2019) (see Scheme 11).

III. Biochemistry of Chl breakdown in higher plants

The pathway of Chl breakdown is nowadays called the 'PAO/phyllobilin' pathway (Hörtensteiner & Kräutler, 2011; Kuai et al., 2018). The name is derived from the key enzyme of the pathway, PAO, which is responsible for the formation of the basic backbone structure of the degradation products of Chl, i.e. the PBs (Kräutler, 2014). The first part of the PAO/phyllobilin pathway describes the enzymatic steps converting colored and phototoxic Chl to a *primary* fluorescent Chl catabolite (*p*FCC) - taking place within the senescent chloroplast. The second part includes FCC-modifying reactions mainly happening in the cytosol followed by the relocalization of the FCCs to the vacuole, where the isomerization to analogous NCCs takes place, thereby causing the loss of the fluorescence property of the FCCs.

A. Colorless, fluorescent Chl catabolites from Chl breakdown in chloroplasts

1. Pheophorbide and other green catabolites with intact Chl macrocycle

a. Chl *b* to Chl *a* conversion

Besides Chl *a*, green algae and plants also contain Chl *b* in their light harvesting complexes (LHCs). However, prior to degradation, Chls must be converted to their '*a*' form since the enzymes downstream in the pathway are specific in accepting this form as substrate (Hörtensteiner, Vicentini, & Matile, 1995; Shimoda, Ito, & Tanaka, 2012) - Chl *b* cannot enter into the degradation pathway unless it is converted to Chl *a*. This is in line with the observation that, with the exception of one NCC from *Arabidopsis* (Müller et al., 2006), PBs derive from Chl *a* (Kräutler, 2016). The conversion of Chl *b* to Chl *a* is catalyzed by two enzymatic steps (Scheme 12). In the first step, Chl *b* reductase (CBR) reduces the C7-formyl group of Chl *b* to 7^1-hydroxy Chl *a* (HOChl *a*) (Scheumann et al., 1999; Tanaka et al., 2011). In the second step, 7^1-hydroxy Chl *a* reductase (HCAR) converts HOChl *a* to Chl *a* (Meguro, Ito, Takabayashi, Tanaka, & Tanaka, 2011).

Arabidopsis has two CBR isoenzymes, i.e. non-yellow coloring 1 (NYC1) and NYC1-like (NOL) (Kusaba et al., 2007; Sato et al., 2009), and both are thought to catalyze the reduction of Chl *b*. However, only the activity of NOL was confirmed in *in vitro* assays. When analyzing the effect of *cbr* mutations in *Arabidopsis in vivo*, *nyc1* mutants show retention of Chl *b* during senescence, whereas Chl *b* levels of *nol* mutants only differ slightly from wild type plants (Horie, Ito, Kusaba, Tanaka, & Tanaka, 2009). An *Arabidopsis nyc1 nol* double mutant shows almost complete suppression of Chl *b* breakdown and a stay-green phenotype during leaf senescence and seed maturation. Interestingly, the double mutant exhibited an unaltered Chl *a*/*b* ratio during vegetative growth, suggesting a crucial role in Chl breakdown but a negligible function in maintaining the Chl *a*/*b* ratio during the vegetative growth phase. This observation is in line with the fact that at least NYC1 is transriptionally upregulated during senescence. The observed stay-green phenotype is explained by the retention of Chl *b,* which results in the stabilization of the LHC proteins to which Chl is bound. This indicates that CBR, thus, indirectly also participates in LHC degradation (Horie et al., 2009).

The second step, catalyzed by HCAR, was characterized in *Arabidopsis*. *In vitro* assays showed the ability of the enzyme to convert 7^1-HOChl *a* to Chl *a*, and in *Arabidopsis* T-DNA insertion mutants for HCAR, accumulation of 7^1-HOChl *a* was observed. Furthermore, the mutant line also accumulated Pheide *a*, a downstream Chl catabolite and substrate of PAO. Interestingly, PAO protein levels were not altered in these plants (Meguro et al., 2011). This together with the fact that in *hcar nyc1 nol* triple mutant plants neither 7^1-HOChl *a* nor Pheide *a* accumulated, suggests a possible interaction between the pigments and enzyme activities (Nagane, Tanaka, & Tanaka, 2010).

b. Magnesium dechelation and dephytylation

The release of the central Mg^{2+}-ion from Chl *a* results in the formation of pheophytin *a* (Phein *a*) (Scheme 12). Non-enzymatic release of Mg^{2+} from Chl *a* occurs slowly under weakly acidic conditions (Saga & Tamiaki, 2012). However, until recently it was unknown which enzyme is responsible for catalyzing this reaction as part of regular Chl breakdown. The puzzle was solved when Shimoda and coworkers identified the enzyme stay-green (SGR) as the Mg-dechelatase involved in senescent leaves (Shimoda, Ito, & Tanaka, 2016).

Even though identification of the molecular function of SGR is only a recent discovery, the stay-green phenotype of *sgr* mutants [also described as *non-yellowing (nye)*] mutants, has been described a long time ago (Hörtensteiner, 2006). The most famous among them is Gregor Mendel's green cotyledon pea (*Pisum sativum*) mutant that was used as a marker for

determining the law of genetics (Mendel, 1866). Defects in orthologous loci were further assigned to cause stay-green phenotypes in *Lolium/Festuca* (Armstead et al., 2006), rice (*Oryza sativa*) (Jiang et al., 2007; Park et al., 2007), *Arabidopsis* (Ren et al., 2007) and over a dozen of other plant species (Hörtensteiner, 2009).

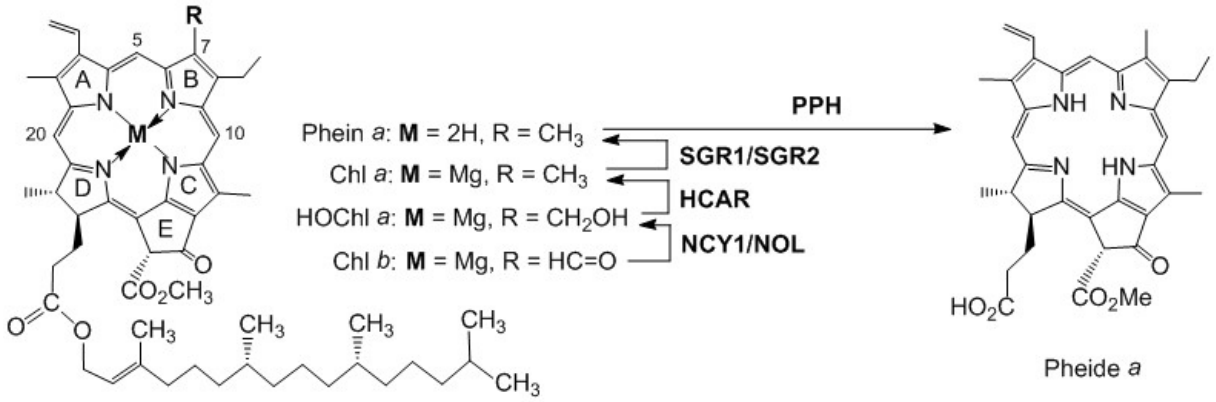

Scheme 12. Outline of the early steps of Chl breakdown in higher plants, depicting chemical structures and critical enzymes (see text and list for abbreviations used).

The *Arabidopsis* genome encodes three SGR proteins, i.e. SGR1 and SGR2, which are highly homologous, as well as SGR-like (SGRL), which is more distantly related (Sakuraba, Kim, Kim, Hörtensteiner, & Paek, 2014b) (also described as NYE1, NYE2 and NYE-like, respectively) (Ren et al., 2007; Wu et al., 2016). SGR1 and 2 share their substrate specificity for Chl, whereas SGRL has a much higher activity for chlorophyllide (Chlide; Chl lacking the phytol chain) – however all three SGRs are specific for the '*a*' form. It has experimentally been shown that SGR acts on free Chl, but also on Chl bound within Chl-protein complexes, i.e. photosystem core complexes and LHCs. Therefore, the role of SGR is not only to catalyze the step in which Chl is committed to degradation, but also to initiate the destabilization of the photosystems (Shimoda et al., 2016). Previously, interaction of SGR with six Chl catabolic enzymes (CCEs), i.e. HCAR, NYC1, NOL, PPH, PAO, and RCCR, together with LHCII was observed, which led to the hypothesis that SGR recruits these CCEs to allow metabolic channeling at the thylakoid membrane during Chl breakdown (Sakuraba, Kim, Yoo, Hörtensteiner, & Paek, 2013; Sakuraba et al., 2012).

Among a collection of *Arabidopsis* mutants deficient in a gene for phytol-hydrolase candidates that were selected based on their predicted chloroplast localization and upregulation during senescence, pheophytinase (PPH) mutants exhibited a stay-green phenotype during induced leaf senescence. In following *in vitro* experiments, the enzyme was shown to specifically hydrolyze Mg^{2+}-free Phein leading to the formation of Pheide (Schelbert et al.,

2009). At about the same time, PPH was independently described in *Arabidopsis* (Ren et al., 2010) and its ortholog in rice (Morita, Sato, Masuda, Nishimura, & Kusaba, 2009). Since then the indispensable function of PPH during Chl breakdown was shown in a range of different plant species, such as Yali pear (*Pyrus x bretschneideri*), tomato (*Solanum lycopersicum*), broccoli (*Brassica oleracea*) and ryegrass (*Lolium perenne*) (Büchert, Civello, & Martínez, 2011; Cheng & Guan, 2014; Guyer et al., 2014; Zhang et al., 2016). Catalytic and structural properties of PPH were recently analyzed in detail (Guyer, Salinger, Krügel, & Hörtensteiner, 2018). Notably, in fruits, redundant phytol-hydrolyzing activity seems to be present: while *pph* mutants of tomato (*Solanum lycopersicum*) showed an impairment in Chl breakdown and accumulated Phein in their senescent leaves, they were still able to degrade Chl in the fruits (Guyer et al., 2014). As a consequence, it was hypothesized that further chloroplastic hydrolases might be involved, however their nature remains elusive. In a genetic screen for heat sensitivity in *Arabidopsis*, chlorophyll dephytylase 1 (CLD1) was identified and proposed to be involved in Chl turnover (Lin, Wu, & Charng, 2016). CLD1 is able to dephytylate both Chl and Phein, but it is unclear so far whether CLD1 might also be involved in leaf senescence- or fruit/seed ripening-related Chl breakdown.

2. *Primary* fluorescent Chl catabolite formation from pheophorbide *a*

For the process of photosynthesis the light absorption capacity of Chl is essential. This is due to the characteristic conjugated π-system of the macroring of the Chls, which still persists in the early Chl catabolites Phein *a* and Pheide *a*. This capacity causes Chl phototoxicity during the degradation of the photosynthetic apparatus. Therefore, the step of the Chl breakdown pathway, in which this feature is lost, can be considered as the key step of Chl detoxification. This is accomplished by the opening of the macrocycle of Pheide *a,* opening a two-step path to the first colorless Chl degradation intermediate *p*FCC. This conversion requires the correlated action of two independent (Hörtensteiner et al., 1995; Rodoni et al., 1997a) but physically interacting enzymes (Pružinská et al., 2007; Sakuraba et al., 2012). The first step is the opening of the porphyrin ring by PAO (Pružinská et al., 2003), thereby producing the hardly detectable RCC (Kräutler et al., 1997; Rodoni et al., 1997a), and the second, the reduction of RCC by RCCR (Wüthrich et al., 2000) (see Scheme 2).

Mutants in either of these two enzymes show a light-dependent accelerated cell death (ACD) phenotype during senescence, and indeed, PAO and RCCR mutants were originally identified as *acd1* and *acd2*, respectively (Greenberg & Ausubel, 1993; Greenberg, Guo, Klessig, & Ausubel, 1994). The observed cell death was proposed to be due to highly photodynamic

properties considered for both Pheide *a* and RCC (Mach, Castillo, Hoogstraten, & Greenberg, 2001; Pružinská et al., 2003; Tanaka, Hirashima, Satoh, & Tanaka, 2003). Interestingly, in addition to light-dependent lesion formation, *pao/acd1*, but not *rccr/acd2* mutants also show light-independent cell death, when leaf senescence is induced in constant darkness (Aubry et al., 2018; Hirashima, Tanaka, & Tanaka, 2009). This led to the hypothesis (Kuai et al., 2018), that Pheide *a* - in addition to being a strong phototoxin (Xodo, Rapozzi, Zacchigna, Drioli, & Zorzet, 2012) - could also act as a cell-death signaling molecule. Christ et al. (2012) showed that Pheide *a* is not able to leave the chloroplast and, therefore, it is considered unlikely that the molecule itself acts as a retrograde chloroplast-to-nucleus signal. Since no further signaling molecules are known in this context, it still remains unclear how light-independent cell death is triggered. Interestingly, in *Arabidopsis pao1* mutant plants, hundreds of genes are differentially expressed already in green tissues before the onset of senescence (Aubry et al., 2018), suggesting an important role of PAO apart from senescence-associated Chl breakdown.

PAO is a Rieske-type mono-oxygenase containing an iron-sulfur cluster, a mononuclear iron center, and two C-terminally located transmembrane domains that anchor the enzyme in the thylakoid membrane with the active site facing to the chloroplast stroma (Pružinská et al., 2003; Sakuraba et al., 2012). It is specific for the '*a*' form of Pheide, which is opened at the C5/C6 position. *In vitro* enzyme assays demonstrated that this activity depends on electron supply by the cofactor ferredoxin (Fd) (Pružinská et al., 2003). Furthermore, in $^{18}O_2$ labeling experiments it was shown that the oxygen incorporated by PAO at the C1 formyl position of *p*FCC is derived from molecular oxygen (Hörtensteiner et al., 1998). The formation of RCC, which is the first linear tetrapyrrolic PB, marks the step when Chl catabolites can pass the chloroplast membrane. This was demonstrated by the finding of RCC-type PBs in the vacuole in *acd2* (Pružinská et al., 2007).

RCCR is a distantly related member of the Fd-dependent bilin reductase family that includes phytochromobilin synthase of higher plants and different phycobilin synthases of red algae and cyanobacteria (Frankenberg, Mukougawa, Kohchi, & Lagarias, 2001). RCCR is localized in the chloroplast stroma (Wüthrich et al., 2000). It reduces the C15/C16 double bond of RCC in a stereospecific fashion, whereby the introduced stereo center at C16 is dependent on the RCCR ortholog. The two different RCCR orthologs, termed type I or type II RCCRs, can be manipulated by an Phe-to-Val exchange at the residue 218, as shown for the *Arabidopsis* RCCR (Pružinská et al., 2007). Later it was shown that this manipulation indeed interferes with the substrate binding pocket of the enzyme (Sugishima et al., 2009; Sugishima et al., 2010). Whether one or the other stereospecific enzyme is present depends on the species. For example,

Arabidopsis has a type I RCCR and, therefore, produces *p*FCC (Mühlecker et al., 1997), while the RCCR from sweet pepper is a type II and produces *epi-p*FCC (Mühlecker et al., 2000). The formation of the *p*FCCs is considered to be the last step of the early PAO/phyllobilin pathway. If not defined otherwise the term *p*FCCs also includes its epimer *epi-p*FCC, as further enzymes are able to use both epimers as substrates. The stereochemistry introduced at the level of the two *p*FCCs is also found in the downstream PBs.

B. Peripheral modifications of fluorescent Chl catabolites

The following enzymatic reactions of the PAO/phyllobilin pathway describe the steps leading to the structural diversity of the final PBs. The sources of these variations are modifications at peripheral side chains on derivatives of the *p*FCCs. One of these modifying reactions still occurs in the chloroplast and - after the release from the chloroplast stroma – the subsequent ones in the cytosol. From then on the downstream fluorescent PBs are termed *m*FCCs or DFCCs. Last, *m*FCCs (and corresponding DFCCs) are transported into the vacuole, where they isomerize non-enzymatically to NCCs (and DNCCs, resepectively) (see Schemes 2 and 5).

The first presumed catabolites derived from Chl were discovered in a senescing variety of *F. pratensis* back in 1987 (Matile et al., 1987). Soon after, pink pigments, were detected in the vacuoles of barley (*Hordeum vulgare*) leaves whose appearance correlated with rates of Chl degradation (Matile, Ginsburg, Schellenberg, & Thomas, 1988). This was followed by further reports on Chl catabolites in different species, but the breakthrough was marked by the structural characterization of a Chl catabolite found in senescent barley leaves, termed *Hv*-NCC-1 (**1**) (Kräutler et al., 1991). This initial discovery allowed conclusions to be drawn concerning enzymatic activities along the breakdown pathway, but also, with subsequent structural elucidations, revealed the catabolite diversity among different species.

The previously described part of the PAO/phyllobilins pathway is widely conserved in plants and the involved enzymes are rather well described. By contrast, much less is known about the enzymes involved in the side chain-modifying reactions described in the following sections. So far, three of these enzymes have been characterized in *Arabidopsis*, i.e. CYP89A9 (Christ et al., 2013), methylesterase 16 (MES16) (Christ et al., 2012) and TIC55 (Hauenstein et al., 2016).

1. Terminal hydroxylation of the ethyl side chain at C3

Hydroxylation at the terminal carbon C3^2 is the first modification of *p*FCCs and furnishes 3^2-hydroxy-*p*FCCs (**3** and ***epi*-3**) within the senescing chloroplast (Hauenstein et al., 2016). A

fluorescent compound that was more polar than the subsequently characterized *p*FCCs, presumably the hydroxy-*p*FCC **3**, was already observed in 1992 in isolated barley chloroplasts (Matile, Schellenberg, & Peisker, 1992). 3^2-hydroxy-*p*FCCs have long evaded characterization (Christ et al., 2012) (Moser et al., 2012) but their intermediary existence has been derived from the occurrence of the corresponding hydroxylated NCCs, for which consistent evidence has been found in all species investigated (Christ et al., 2016; Curty & Engel, 1996; Kräutler, 2016; Roca et al., 2018). The common occurrence of the hydroxylation and its localization within the plastid (Hauenstein et al., 2016) connects this reaction to the first part of the PAO/phyllobilin pathway and, thus, 3^2-hydroxy-*p*FCCs can be considered 'secondary' FCCs (*s*FCCs). In senescent wild type leaves of *Arabidopsis*, sFCC (=3^2-hydroxy-*p*FCC) is the precursor of all hydroxylated PBs which compose more than 50% of the catabolites. Only recently the responsible enzyme catalyzing the $C3^2$ hydroxylation of *p*FCC in *Arabidopsis* was characterized and identified as TIC55 (Hauenstein et al., 2016). TIC55 belongs to the class of Rieske-type mono-oxygenases, like PAO. It was shown to catalyze the $C3^2$ hydroxylation of *p*FCC *in vitro* in an Fd-dependent way producing 3^2-hydroxy-*p*FCC (*s*FCC). 3^2-hydroxylated PBs are completely absent in senescent leaves of *tic55* mutants, demonstrating the requirement of TIC55 for their production. Apart from the clear phenotype in the catabolite profile, *tic55* mutants show no other physiological differences to wild type plants (Hauenstein et al., 2016). Previously, TIC55 was assigned to be a potential component of the protein import machinery at the inner chloroplast membrane with a speculated role in redox sensing (Balsera, Soll, & Buchanan, 2010; Bartsch et al., 2008; Calibe et al., 1997). However, experimental evidence for this function is missing (Boij, Patel, Garcia, Jarvis, & Aronsson, 2009).

2. O-glycosylation and malonylation reactions

After the release of *p*FCC or its hydroxylated form from the plastid to the cytosol, further species-specific side chain modifications occur effectively. The hydroxyethyl side chain at C3 of 3^2-hydroxy-*p*FCCs can subsequently be glucosylated and/or malonylated, as found in some species such as *Arabidopsis*, tobacco (*Nicotiana rustica*) (Berghold, Eichmüller, Hörtensteiner, & Kräutler, 2004) and oilseed rape (Mühlecker et al., 1993), as well as in ripe fruits, such as apples and pears (Müller et al., 2007), loquat (*Eriobotrya japonica*) and quince (*Cydonia oblonga*) (Rios et al., 2014a; Rios et al., 2014b). The relative amount of glucosylated catabolites varies greatly across species. In different *Arabidopsis* ecotypes only around 5% of the catabolites are glucosylated (Christ et al., 2016), whereas in tobacco all of the known Chl catabolites are glucosylated or additionally malonylated (Berghold et al., 2004). Although

malonyltransferase activity has been characterized in oilseed rape (Hörtensteiner, 1998), the responsible enzyme for malonylation still remains unknown. For glucosylation, it has been speculated that UDP-dependent glycosyltransferases might play a role, since they are known to catalyze the addition of glucose to hydroxyl groups. However, so far none of the UDP-dependent glycosyltransferases could be assigned to this function. Based on the fact that isolated senescing chloroplasts do not accumulate glucosylated FCCs and that *tic55* mutants lack glucosylated phyllobilanes (NCCs and DNCCs) (Hauenstein et al., 2016), the proposed glycosyltransferases are likely cytosolic enzymes and FCC hydroxylation is an obvious prerequisite for subsequent glucosylation.

3. Oxidative deformylation to dioxobilin-type Chl catabolites

Deformylation at C1 leads to the conversion of FCCs to their respective dioxobilin-type analogs, the DFCCs. Respective nonfluorescent DNCCs had originally been identified in barley (Losey & Engel, 2001) but were thought to be oxidation products of NCCs, probably for a long time, even though they are the major Chl catabolites accounting for over 90% of all PBs in this species (Christ et al., 2013; Süssenbacher et al., 2014). Only in 2013 DNCCs were described in the published literature as the main products of Chl breakdown in *Arabidopsis* and the responsible enzyme activity identified in the cytosol (Christ et al., 2013). DNCC formation in senescent leaves was inhibited in a carbon monoxide-enriched atmosphere, indicating CYPs could be responsible for deformylation. Based on these results, CYP gene candidates were selected and respective mutants screened for altered catabolite profiles. It was found that *cyp89a9* mutants are devoid of DNCCs, while accumulating accordingly more NCCs. Further *in vitro* enzyme assays confirmed this candidate (Christ et al., 2013). CYP89A9 localizes to the ER, and oxidatively deformylates FCCs, but not NCCs. The occurrence of DNCCs and NCCs varies among different plant species (Das, Christ, & Hörtensteiner, 2018). In contrast to *Arabidopsis*, which accumulates both types of PBs, in *C. japonicum* exclusively NCCs are found (Curty & Engel, 1996; Oberhuber et al., 2003), while in Norway maple one single DNCC accumulates, but no NCCs (Müller et al., 2011).

4. Hydrolysis of the methyl ester function

MES16 catalyzes the $C8^2$ carboxymethyl group demethylation of PBs in *Arabidopsis.* As revealed by the recently published crystal structure, it belongs to the α/β-hydrolase protein superfamily (Li & Pu, 2016). It was experimentally shown that the natural substrates of MES16 are cytosolic fluorescent PBs, even though mistargeted chloroplast-localized MES16 was able

to convert Pheide *a* to *py*Pheide *a* in a *pao* mutant background (Christ et al., 2012). In senescent *mes16* mutant leaves, isomerization of FCCs (and, presumably, DFCCs) to corresponding phyllobilanes was slowed down. This led to the accumulation of fluorescent PBs in the vacuole, which was also visible under UV light as it caused senescent leaves of *mes16* to fluoresce (Christ et al., 2012). The demethylation of PBs is, as the deformylation, highly species-specific. Interestingly, even within the species of *Arabidopsis*, the Landsberg *erecta* (L*er*) ecotype, seems to be a natural *mes16* mutant. Of 18 analyzed *Arabidopsis* ecotypes all except L*er* showed demethylated PBs of close to 100% (Christ et al., 2016; Christ et al., 2012). However, this may only be an artifact, since it was shown that many lab strains of L*er* are derived from an ethan-methylsulfonic acid-induced mutagenesis event that explains the occurrence of many single nucleotide polymorphisms in this accession (Zapata et al., 2016).

Besides its role in Chl breakdown, MES16 also accepts methyl-indole acetic acid as a substrate (Abbas et al., 2018; Christ et al., 2012; Yang et al., 2008). Together with the finding of its upregulation during the night this led to the hypothesis that MES16 could play a role in auxin activation during nocturnal growth (S. Hörtensteiner, unpublished).

5. Dihydroxylation of the vinyl group at C18

C18-dihydroxylated PBs have been identified in many plants; in particular, they have been found in all grass species analysed to date (Berghold, Müller, Ulrich, Hörtensteiner, & Kräutler, 2006; Das et al., 2018; Kräutler et al., 1991), while they are absent from several families of angiosperms such as the Brassicaceae (Christ et al., 2016; Mühlecker & Kräutler, 1996; Pružinská et al., 2005). This indicates the presence of a respective dihydroxylating activity in only certain plant clades. $^{18}O_2$-labeling experiments showed that both oxygen atoms incorporated into the C18-dihydroxyethyl group are derived from molecular oxygen, indicating that the responsible enzyme(s) could be a dioxygenase (Das et al., 2018). However, the molecular identity of such a dioxygenase remains elusive.

6. Esterification at the propionyl group

Typical FCCs usually only exist fleetingly before they are further converted to NCCs (Oberhuber et al., 2003). However, banana and peace lily accumulate hypermodified blue fluorescent catabolites, i.e. *hm*FCCs, in their senescent leaves (Banala et al., 2010) and also in the ripe banana fruit peel (Moser et al., 2008a; Moser et al., 2009). The accumulation of *hm*FCCs in ripe banana peels was shown to be the dominant cause of their fluorescent blue glow (Moser et al., 2008a; Moser et al., 2009) The persistency of *hm*FCCs is caused by the

esterification of their propionic acid group with different functional groups, such as daucyl, glucosyl, digalactosyl-glyceryl, or glucosyl-(dihydroxyphenyl) ethyl, which greatly interferes with the FCC-to-NCC isomerization (Oberhuber et al., 2008). In the exceptional bicycloglycosidic PBs **13**, **14** and **25** (see above and Schemes 3 ,4 and 6), both esterification and glycosidation are present. However, the mechanisms of glycosylation and propionate esterification remain unsolved and require the identification of the respective enzyme(s) catalyzing these modifications.

C. Core transformations of fluorescent Chl catabolites

1. Isomerization to nonfluorescent Chl catabolites

As described in section B, the typical FCCs are prone to spontaneous and stereoselective isomerization to the apparently more stable corresponding NCCs (see Scheme 5) (Oberhuber et al., 2003). Hence, this chemical reaction has been proposed to account for the formation of NCCs and, indeed, there is no evidence for an enzyme catalyzing an FCC to NCC isomerization (Hörtensteiner & Kräutler, 2011; Kräutler, 2016; Kuai et al., 2018). Consistent with the subcellular location of NCCs (Hinder et al., 1996), transport of FCCs into the acidic vacuole and their chemical isomerization to NCCs has been accepted as the biochemical model of the NCC formation step in senescent leaves (Kräutler, 2016). A related mechanism has been deduced to concern the formation of DNCCs from the corresponding DFCCs (Süssenbacher et al., 2015a).

2. Carbon skeleton rearrangement and pyro formation

Recent analysis of the fern *P. aquilinum* revealed an unprecedented type of PBs, which were classified as *i*PBons (Erhart et al., 2018b). These novel PBs are devoid of the typical carboxylic acid or ester function at $C8^2$ classifying them as *pyro*-PBs. So far, evidence for the natural occurrence of *py*NCCs was missing and explained by the surprising resistance of NCCs for the loss of this carboxyl unit (Li et al., 2018). Thus, pyro formation may occur on the level of Pheide *a*; hence inside plastids. However, this would require a MES16-like activity inside the plastid as well (see above) (Christ et al., 2012). Alternatively, *P. aquilinum* may possess a so called ‘demethoxycarbonylase’, as described in the green alga *Chlamydomonas reinhardtii* (Suzuki, Doi, & Shioi, 2002) and suggested to be able to cleave the entire carboxymethyl group. Possibly, such an enzyme might act even at a later stage of Chl breakdown, i.e. on the level of a linear tetrapyrrole, but a corrsponding activity has not been identified.

Furthermore, *i*PBons show a unique carbon skeleton rearrangement, where the connection of ring A to ring B, which is usually the C5/C6 carbon bond, is shifted to a C5/C7 bond (Erhart et al., 2018b). Except this difference, the carbon backbone is identical to the known type-I Chl catabolites and it has been presumed that these *i*PBons derive from a precursor PB generated in the 'early' part of the PAO/phyllobilin pathway (Erhart et al., 2018b). Although, both pyro formation and carbon skeleton shift were deduced from the structures of the *i*PBons, they probably are not synchronized. However, hydroxylation at C6 is a prerequisiste for the ring A migration and may occur on the level of an FCC (Erhart et al., 2018b). The nature of such a novel enzyme remains elusive. From an evolutionary point of view carbon skeleton shift and pyro formation are interesting, as they occur in lower plants, such as ferns and some Gymnosperms, including *Ginkgo biloba* (Erhart et al., 2018b) (T. Erhart, T. Müller and B. Kräutler, unpublished; M. Hauenstein and S. Hörtensteiner, unpublished), but have been lost during the evolution of the angiosperms.

IV. Biology of Chl breakdown in plants

A. Subcellular localization of enzymes involved in Chl breakdown and catabolite transport

Already in 1988, when Chl catabolites were detected in senescent barley leaves, it was shown that the majority of the catabolites are present in the vacuolar fraction (Matile et al., 1988), implying the vacuole to be the typical place for their end storage (Matile, Hörtensteiner, Thomas, & Kräutler, 1996). Later this was also confirmed in other plant species (Christ et al., 2012; Hinder et al., 1996; Pružinská et al., 2007). Thus, typical Chl breakdown starts in senescing chloroplasts and ends inside the vacuole. A combination of biochemical approaches, cell fractionation studies and, recently, molecular cloning and localization studies of CCEs unvovered a cellular topology of Chl breakdown as depicted in Figure 1. The first part of the PAO/phyllobilin pathway is localized inside the plastid. Protein-protein interaction analysis and localization studies using green fluorescent protein fusions, indicated that the enzymes of the first part of the pathway required to form *p*FCC, i.e. NYC1, NOL, HCAR, SGR, PPH, PAO and RCCR, likely form a protein complex at the thylakoid membrane, which was considered to be important for metabolic chanelling of otherwise potentially phototoxic Chl breakdown intermediates (Sakuraba et al., 2013; Sakuraba et al., 2012). The localization of TIC55 is distinct from the other chloroplast-located CCEs, i.e. in the chloroplast envelope. Whether this links PB hydroxylation with FCC export from the plastid remains to be investigated. Based on the fact that Chl breakdown is not hampered in *tic55* mutants, it seems likely that catabolite

export also occurs in the absence of TIC55 (Hauenstein et al., 2016). In *Arabidopsis*, additional *p*FCC-modifying CCEs are located outside the plastid, i.e. in the cytosol (MES16) or attached to the ER (CYP89A9), and it is likely to assume that also further activities, like $O3^3$-glucosylation, $O3^3$-malonylation and C18 vinyl group dihydroxylation, occur in the cytosol.

Figure 1 here

Given the fact that *p*FCCs/*s*FCCs are formed inside the plastid and that the isomerization process, which converts FCCs and DFCCs into their respective phyllobilane isomers (NCCs and DNCCs), happens non-enzymatically in an acidic environment (Oberhuber et al., 2003; Oberhuber et al., 2008; Süssenbacher et al., 2015a) - such as found inside the vacuole (Christ et al., 2013; Oberhuber et al., 2003), two membrane transport steps could be postulated, i.e. *p*FCC/sFCC export from the chloroplast and subsequent import of FCCs and DFCCs into the vacuole. Using isolated senescent chloroplasts of barley, Matile et al. (1992) demonstrated that export of the fluorescent presumed Chl catabolites requires supply and hydrolysis of ATP. However, the nature of transport remains unknown and up to now, envelope Chl catabolite transporters have not been identified at the molecular level. Nevertheless, based on the subcellular accumulation of intermediates in respective Chl breakdown mutants (Christ et al., 2012; Pružinská et al., 2007) it can be concluded that the envelope transporter(s) likely accepts linear tetrapyrroles, i.e. RCC- or FCC-type PBs as substrate, but not porphyrins, like Pheide *a*.

In contrast to chloroplast export, it was demonstrated that transport of Chl catabolites into isolated barley vacuoles is ATP-dependent. Inhibition studies of the transport indicated it to be a primary active process and, therefore, ATP-binding cassette (ABC) transporters are likely candidates for PB uptake into the vacuole (Hinder et al., 1996). Indeed, NCC transport could be demonstrated in yeast (*Saccharomyces cerevisiae*), which heterologously expressed ABCC2 and ABCC3 transporters of *Arabidopsis* (Lu et al., 1998; Tommasini et al., 1998). However, the characterization of ABC transporters is aggravated by their high substrate redundancy (Kang et al., 2011) and, therefore, the responsible transporter(s) of Chl catabolites *in vivo* has/have not been identified yet.

B. Regulatory aspects of Chl breakdown

Senescence in plants generally results in an increase of catabolic and a decrease of anabolic processes ultimately leading to cell death at a cellular, tissue, organ, or organismal level (Lim, Kim, & Nam, 2007). The complex molecular mechanisms involved in this process are

orchestrated by internal or external factors. Important internal factors are stages of plant development and/or the action of phytohormones (Zhu, Chen, Qiu, & Kuai, 2017). External factors can be divided into biotic ones, such as pathogens, or abiotic ones, which include environmental stresses like light, temperature, drought, ozone or nutrient deficiency (Lim et al., 2007). The transcriptional regulation of senescence and of Chl breakdown are often mediated by the same factors. The following sections outline the current knowledge of regulatory cues of Chl breakdown, i.e. the link and impact of transcriptional control of Chl catabolic genes (CCGs) encoding respective CCEs.

1. Ethylene

Ethylene is known for a long time as one of the major inducers of leaf senescence, fruit ripening and flower senescence (Abeles et al., 1988; Bleecker, Estelle, Somerville, & Kende, 1988; Chao et al., 1997). Likewise, ethylene-triggered Chl breakdown as the cause for the degreening process during leaf senescence and fruit maturation has been described (Azoulay Shemer et al., 2008; Cheng & Guan, 2014; Yin et al., 2016). Only recently the underlying molecular genetic mechanisms, which link ethylene to Chl breakdown during senescence have been elucidated. Generally, ethylene acts as a promoter of CCG expression through the transcription factors (TFs) EIN3 (ethylene insensitive 3) and ORE1 (oresara 1). EIN3 was shown to physically bind to the promoters of the genes encoding NYE1, NYC1 and PAO to activate their expression. ORE1, which is a direct target of EIN3 is also able to bind promoter regions of *NYE1*, *NYC1*, *NOL* and *PAO*, thereby activates their expression, and, in addition, increases ethylene production by inducing ACS2 (aminocyclopropane-1-carboxylic acid synthase 2), a major ethylene biosynthesis gene. Taken together EIN3, ORE1, and ACS2 create a feed-forward loop that regulates ethylene-mediated Chl breakdown during leaf senescence in *Arabidopsis* (Qiu et al., 2015). For Chl breakdown in ripening fruits, an ethylene-responsive factor was reported, probably acting *via* induction of *PPH* expression (Yin et al., 2016).

2. Abscisic acid

Involvement of abscisic acid (ABA) in stress-induced leaf senescence and seed maturation is deduced from a significant increase of ABA during these processes (Breeze et al., 2011; Gepstein & Thimann, 1980; Liu, Longhurst, Talavera-Rauh, Hokin, & Barton, 2016). The TFs ABF (ABA-responsive element-binding factor) and RAV1 (related to ABA-insensitive 3/viviparous 1) both upregulate expression of senescence-associated genes *via* ORE1, which connects the signaling pathway of ABA to ethylene signaling. It has been demonstrated that

changes in ABA levels, i.e. either modified endogenous levels or exogenous application, affect expression of CCGs (Raab et al., 2009; Takasaki et al., 2015; Ye et al., 2017). The molecular genetic cause for this altered expression levels were recently described. The two TFs ABI5 (ABA insensitive 5) and EEL (enhanced EM level), both of which act in the ABA signaling pathway, directly upregulate *NYE1* and *NYC1* (Sakuraba et al., 2014a). A further component of the ABA signaling pathway, NAC016 [NAM (no apical meristem), ATAF1/2, CUC (cup-shaped cotyledon) 16], was shown to directly activate *NYE1* expression (Sakuraba, Han, Lee, Hörtensteiner, & Paek, 2016). Furthermore, *NYE1/2*, *NYC1* and *PAO* are activated during natural and ABA-triggered leaf senescence by ABF2/3/4 (Gao et al. 2016). During seed maturation the TF ABI3 seems to play an important role by regulating *NYE1/2* expression (Delmas et al., 2013).

3. Jasmonates

Already in 1980, methyl jasmonate (MeJA) and its precursor jasmonic acid (JA) were shown to be strong inducers of plant senescence (Ueda & Kato, 1980). He et al. (2002) found that during leaf senescence in *Arabidopsis* measured JA levels were four-fold higher compared to non-senescing leaves, in line with the finding that during senescence JA biosynthesis-related genes are differentially activated. Furthermore, it was demonstrated that exogenous application of JA promotes senescence (He et al., 2002). Later, components of JA-induced senescence have been identified (Jiang, Liang, Yang, & Yu, 2014; Qi et al., 2015; Shan et al., 2011). How JA signaling impacts regulation of Chl degradation on the molecular genetic level was reported recently (Zhu et al., 2015). It was demonstrated that MYC (myelocytomatosis) proteins (MYC2/3/4) - key players in JA signaling - act as direct transcriptional regulators of *PAO* and, furthermore, are able to bind to the promoter regions of *NYE1* and *NYC1* and to regulate their expression. In the same study, it was shown that ANAC (*Arabidopsis* NAC) proteins (ANAC019/055/072), downstream targets of the MYCs in the JA signaling pathway, are able to directly activate *NYE1/2* and *NYC1*. Protein-protein interaction between ANAC019 and MYC2 causes upregulation of the expression of *NYE1* (Zhu et al., 2015).

4. Light

Already 35 years ago, light was shown to act as an environmental cue of senescence (Biswal & Biswal, 1984), i.e. red and far-red light pulses retarded and re-stimulated, respectively, leaf senescence. Also the fact that prolonged absence of light leads to senescence in plants is widely used to study senescence and Chl breakdown. This light-dependent signaling is mediated by

phytochromes, which are important light receptors found in plants (Biswal & Biswal, 1984; Liebsch & Keech, 2016). Light impulses sensed by phytochromes are transmitted by PIFs (phytochrome-interacting factors), which are the major TFs controlling dark-induced senescence, with PIF3/4 and 5 acting as positive regulators of leaf senescence. PIF4 and 5 target ABI5/EEL and EIN3, which directly upregulate *NYE1* and *NYC1* (Sakuraba et al., 2014a). Additionally, EIN3 also directly targets ORE1 and thereby activates expression of *NYE1*, *NYC1*, *NOL* and *PAO* as described above in the context of ethylene signaling.

C. Significance of chlorophyll breakdown in plants

While senescence processes in different plant organs such as leaves, fruits and seeds lead to distinct ultrastructural changes within the specific organ tissue, it has been shown that the expression pattern of a very wide range of genes is regulated in an analogous way (Krupinska, Biswal, & Biswal, 2013). These senescence-associated genes encode proteins involved in macromolecule degradation, removal of oxidative metabolites, induction of defense mechanisms, and signaling and regulatory events (Gepstein et al., 2003). Recycling and detoxification are seen as the main consequences of structural and biochemical changes occurring in leaves and fruits prior to their shedding. Visually they share the most obvious signs of the so-called senescence syndrome (Lim et al., 2007), i.e. the degradation of Chl.

1. Chl breakdown and leaf senescence

Senescence in leaves usually progresses in an age-dependent manner or is seasonally induced by short day length in deciduous plants. But senescence can also be a premature response to different biotic and abiotic stresses, such as lack of light, drought or pathogen attack (Guo & Gan, 2012; Lim et al., 2007). In leaves, signs of senescence usually start from the tip and progress to the base, and within the mesophyll from the inside towards the epidermis, excluding tissues along vascular bundles (Inada, Sakai, Kuroiwa, & Kuroiwa, 1998), or occur locally upon pathogen infection. In *Arabidopsis*, infection with *Pseudomonas syringae* was shown to lead to senescence-associated Chl breakdown (Mecey et al., 2011; Mur et al., 2010). In terms of Chl breakdown, the leaf is the best-characterized plant organ, since it served as a starting point for research and characterization of the PAO/phyllobilin pathway.

2. Chl breakdown and fruit ripening

The ripening process of fruits relates to senescence processes. Ripening of dry fruits, as found, for example, in the siliques of *Arabidopsis*, is much more similar to leaf senescence

(Mizzotti et al., 2018), while in fleshy fruits, ripening is accompanied by many more physiological changes, such as carotenoid and anthocyan synthesis, pericarp softening, cell wall degeneration and starch to sugar conversion (Gomez, Vera-Sirera, & Perez-Amador, 2014). In fleshy fruits, such as tomato, the color change is caused by the transition of chloroplasts into chromoplasts. This differentiation includes the lysis of grana stacks and thylakoid membranes as well as the synthesis of new membranes derived from the former inner plastid membrane, which become the specialized site for carotenoid synthesis (Barsan et al., 2012; Kahlau & Bock, 2008). Only when Chl is broken down, previously hidden and newly synthesized carotenoids and anthocyans get unmasked, revealing the eye-catching colors of fruits. It was demonstrated that fruit color is dependent on abiotic factors, but also a result of evolutionary adaption to the visual detection by specific seed-dispersing animals (Valenta et al., 2018). Additionally, it was shown that colored Chl catabolites, i.e. YCCs and PiCCs, contribute to the color of senescent leaves or ripened fruits (Moser et al., 2008b; Ulrich et al., 2011), and NCCs in ripe fruits were demonstrated to be powerful antioxidants (Müller et al., 2007).

However, the underlying biochemical processes of Chl breakdown in fruits are not entirely resolved. CCEs known to be involved in Chl breakdown in leaves have also been identified in fruit proteomic studies (Barsan et al., 2010; Li Z. P. et al., 2017; Wang et al., 2013). While in some fruits, such as apple (Malus *domestica*) and pear (*Pyrus communis*), chlorophyll is broken down to PBs that are identical to those from respective senescent leaves (Müller et al., 2007), in other species there are some inconsistencies regarding Chl breakdown in leaves compared to fruits. As an example, different PBs are found in ripening banana fruit (Moser et al., 2008a; Moser et al., 2009; Moser et al., 2012) and their senescing leaves (Banala et al., 2010). Furthermore, *pph* mutants in *Arabidopsis* and tomato exhibit a clear stay-green phenotype during leaf senescence, in contrast to their fruits and seeds (Guyer et al., 2014; Zhang et al., 2014). However, at least in *Arabidopsis pph*, lower amounts of catabolites and higher amounts of retained Chl were observed in the siliques as compared to wild type (D. Menghini and S. Hörtensteiner, unpublished). This demonstrates the involvement of PPH in the breakdown of Chl in the generative tissue, but also suggests the involvement of further hydrolytic activities. For ripening of citrus fruits, chlorophyllases have been proposed to be involved in dephytylation (Azoulay-Shemer et al., 2011; Azoulay Shemer et al., 2008). Furthermore, in contrast to senescent leaves, *Arabidopsis pao* mutants do not show retention of green color in seeds and siliques. Even though the seeds appeared to have a wild type phenotype with regard to their color, they do not accumulate any PBs as analyzed by LC-MS, revealing that also in seeds,

PAO absence results in an entire blockage of the pathway (D. Menghini and S. Hörtensteiner, unpublished).

3. Chl breakdown and seed development

Development of seeds can be described in two phases, the morphogenesis phase, involving the development of the embryo and the endosperm; and the maturation phase, in which desiccation tolerance and seed dormancy are established. This phase involves senescence processes where, particularly in the late phase, Chl is rapidly degraded (Li, Ban, Limwachiranon, & Luo, 2017). Plant varieties with a green seed phenotype have been known for a long time; most famously, Mendel's green cotyledon mutant in pea, but also in certain varieties of other species, such as soybean (*Glycine max*) and *Arabidopsis*, in which NYE genes were shown to be mutated (Fang et al., 2014; Sato, Morita, Nishimura, Yamaguchi, & Kusaba, 2007). NOL was also shown to be involved in Chl degradation in seeds, which is in fact crucial for seed storability (Nakajima, Ito, Tanaka, & Tanaka, 2012). This demonstrates the involvement of the enzymes of the PAO/phyllobilin pathway that have been characterized in leaves. While it is clear that Chl breakdown in leaves and seeds share biochemical characteristics similar to fruits, there are also some inconsistencies. Thus, leaves of the *Arabidopsis nye1* mutant shows a stay-green phenotype, while during seed maturation Chl is only retained in a *nye1 nye2* double mutant, possibly due to tissue-specific redundancy (Delmas et al., 2013; Wu et al., 2016). Furthermore, it was shown that distribution of differentially modified PB is not the same in leaves and seeds, presumably due to different activities of the phyllobilin-modifying enzymes (D. Menghini and S. Hörtensteiner, unpublished).

D. Evolutionary aspects of Chl breakdown

Angiosperms, as the most diverse division of the plant kingdom, have been the main focus of studies on Chl breakdown (Hörtensteiner & Kräutler, 2011; Kuai et al., 2018). The structure-based information about Chl catabolites is therefore almost exclusively restricted to the ones identified in angiosperms (Kräutler, 2016). So far, there are no published records of PBs in gymnosperms and mosses. However, only very recently the knowledge gap of PBs in ferns was filled with the first report on *i*PBons in *P. aquilinum*, revealing a novel type of Chl catabolites with a rearranged carbon backbone (Erhart et al., 2018b). Interestingly, similar catabolites are also found in the primitive gymnosperm *Ginkgo biloba* (Erhart et al., 2018b) (T. Erhart, T. Müller and B. Kräutler, unpublished; M. Hauenstein and S. Hörtensteiner, unpublished). As these Chl catabolites seem to stem from a precursor of the PAO/phyllobilin pathway, the earlier

hypothesis is supported that this pathway is highly conserved among land plants (Hörtensteiner, 2013; Thomas, Huang, Young, & Ougham, 2009).

Phylogenetic analysis demonstrated that CCEs, like NYEs, PPH, PAO, RCCR and TIC55, are highly conserved among them, whereby gene homology decreases in more basal photosynthetic organisms (Hauenstein et al., 2016; Pružinská et al., 2007; Schelbert et al., 2009; Thomas et al., 2009). Functional parallels of RCCR have been demonstrated in the Gymnosperm *Pinus taeda*, the liverwort *Marchantia polymorpha*, and the bryophyte *Physcomitrella patens* (Pružinská et al., 2007). Based on these findings and despite the incomplete evidence of PBs in land plants (Erhart et al., 2018b), it is assumed that the biochemical processes of the PAO/phyllobilin pathway are ubiquitous (Kuai et al., 2018).

The early part of the PAO/phyllobilin pathway seems to have established even further back on an evolutionary time scale, i.e. already before the evolution of land plants. The green alga *A. protothecoides* is known to be able to degrade Chl under N-limited, heterotrophic conditions in the dark (Curty & Engel, 1996). However, in contrast to land plants, *A. protothecoides* degrades Chl only to the stage of red catabolites (related to RCC), seemingly requiring the same biochemical processes as described for angiosperms (Curty, Engel, & Gossauer, 1995). The formed red catabolites are then excreted into the surrounding medium. A different way to eliminate phototoxic Chl catabolites, i.e. disposal in the vacuole, was only required when plants invaded terrestrial habitats and where no longer surrounded by aqueous environments (Hörtensteiner, 2006). In line with this hypothesis is the finding that RCCR proved absent from algae based on *in silico* predictions (Gao et al., 2014) (S. Aubry and S. Hörtensteiner, unpublished). Homologues of the upstream enzymes have not been characterized yet. The most similar PAO-like enzyme exhibits 31% sequence identity to the one of *Arabidopsis* and functional validation is required.

In contrast to the first part of the PAO/phyllobilin pathway, which seems to be highly conserved, the second part - mainly describing the side chain modifications of PBs (Kräutler, 2016) - is highly diverse between species. Since some of these modifications of PBs do not seem to be essential for the plant, i.e. obvious phenotypes of missing in respective *Arabidopsis* mutants (Christ et al., 2012; Christ et al., 2013; Hauenstein et al., 2016), their physiological function and the reason for their diversity in different species is still an enigma. Using the catabolite profiles of all plants identified so far and putting them into a phylogenetic context, may allow tracing back the arise of these side chain-modifying activities to gain information on the specific recruitment of respective CCEs for Chl breakdown. Whether the known PBs represent the end stage of Chl breakdown or if degradation occurs beyond them in viable leaf

tissue is not clear yet. It has been reported that the amount of degraded Chl does not always correlate with the amount of accumulated PBs (Berghold et al., 2002; Christ et al., 2016; Das et al., 2018; Kräutler et al., 1992; Losey & Engel, 2001). Catabolite analysis of leaves of a *Nicotiana benthamiana* plant that were selected along the stem, i.e. represent a senescence gradient, uncovered a peak of PB in mid-senescent leaves, which decreased again in the oldest leaves (M. Hauenstein and S. Hörtensteiner, unpublished). Furthermore, in senescent barley leaves, monopyrrolic compounds inferred to be Chl catabolites were identified (Suzuki & Shioi, 1999). Clearly, further degradation of Chl beyond the stage of the known PBs is rather likely and its elucidation remains to be a challenge (Kräutler, 2016; Li et al., 2019) (C. J. Li & B. Kräutler, unpublished).

V. Conclusions and Outlook

The fate of Chl during breakdown, considered an 'enigma' until about 30 years ago (Hendry et al., 1987), has been largely resolved based on the compiled research of the last almost 30 years, which contributed to the biochemical, molecular and structural elucidation of Chl breakdown, now termed the PAO/phyllobilin pathway (Kräutler & Hörtensteiner, 2014), and its degradation products. The core pathway, i.e. the consecutive conversion of Chl to non-phototoxic intermediates within the chloroplast, was finally resolved with the recent discovery of the Mg dechelatase activity of SGR (Shimoda et al., 2016). This part of the degradation pathway is thought to be widely conserved in photosynthetically active organisms, down to basic unicellular algae, such as *A. protothecoides* (Matile, Hörtensteiner, & Thomas, 1999; Thomas et al., 2009), implying the importance of Chl degradation as detoxification process, in order to protect a cell from photooxidative damage by Chl (Hörtensteiner, 2004; Hörtensteiner & Kräutler, 2011). Interestingly, with the colonialization of terrestrial habitats, plants acquired further processing steps in order to store the accumulating Chl catabolites within the cell (Hinder et al., 1996; Oberhuber et al., 2003), *versus* excretion of RCC-like compounds in the surrounding aqueous environment as in *A. protothecoides* (Engel et al., 1996). These processing steps in higher land plants are further modifications of the first colorless degradation intermediate *p*FCC. These 'late' Chl degradation processes create the large number of different PBs known to date (Kräutler, 2016). This variation is in clear contrast to the high conservation of the core first part of Chl degradation and is much less well understood. The only molecularly identified enzymes of this part of Chl breakdown so far are CYP89A9, MES16 and TIC55 from *Arabidopsis*. Their discovery will allow creating a *cyp89a9 mes16 tic55* triple mutant in the future to allow investigating potential biological roles of the modified downstream PBs.

One of the future challenges regarding Chl breakdown is to bring the occurrence of the PAO/phyllobilin pathway in an evolutionary context, i.e. to answer the standing questions, when during evolution the pathway emerged. Data about the conservation and diversity of parts of the pathway (Gray et al., 2004; Thomas et al., 2009) let us draw the picture of a core first part that takes place within the chloroplast and, thus, likely evolved from genes that were present in the cyanobacterial endosymbiont; and of a second, much more diverse part, i.e. reactions of PB side chain modifications. Particularly, the evolutionary emergence of the latter – combined with a possible physiological relevance of PBs with these modifications (Kräutler, 2016; Moser et al., 2012; Vergeiner et al., 2013) – will be most challenging.

The observation is intriguing that abundance of PBs is low in senescent leaf tissue in many plant species despite the obvious visible signs of Chl breakdown (Das et al., 2018). This raises interesting questions regarding the final fate of Chl during breakdown, which 30 years ago was still enigmatic in many respects (Matile et al., 1987). Although our understanding of Chl breakdown has substantially increased since then (Kräutler, 2016; Kuai et al., 2018), we still may be 'naïve' about nature's ability of diversification. This is seen by the fact that successively new types of colorless breakdown products were identified since the first structural description of an NCC almost 30 years ago (Kräutler, 2016; Kräutler et al., 1991), in particular, the *hm*FCCs (Moser et al., 2008a), the DNCCs (Christ et al., 2013; Losey & Engel, 2001) and the recently identified *i*PBons (Erhart et al., 2018b), but also minor forms, such as the brightly colored YCCs and PiCCs (Moser et al., 2008b; Ulrich et al., 2011).

Nevertheless, the key step to all these (downstream) Chl catabolites, is PAO (Pružinská et al., 2003), making it unlikely that, in higher plants, other pathways of Chl degradation that have been considered in the past (Hynninen, Kaartinen, & Kolehmainen, 2010; Johnson-Flanagan & Spencer, 1996; Matile, 1980) indeed exist besides the PAO/phyllobilin pathway. A notable diversification is the detection in heterotrophic protists of Chl breakdown (and detoxification) through the formation of an enol between the C17 propionic acid and ring E of Pheide *a* (Kashiyama et al., 2012; Kashiyama et al., 2013). These so-called 13^2,17^3-cyclopheophorbide enols are, in contrast to Chl, Phein and Pheide, nonfluorescent and do not produce singlet oxygen upon light excitation (Falk, Hoornaert, Isenring, & Eschenmoser, 1975). The biochemistry of the formation of these compounds is entirely unknown (Kashiyama & Tamiaki, 2014).

PBs display a remarkable diversity of structural properties, contrasting with the lack of knowledge of the phyllobilin-modifiying enzymes, including those that achieve C18 dihydroxylation, $O3^3$ glucosylation and/or malonylation, as well as the remarkable $C12^3$

hypermodifications. PBs are also ubiquitous in nature, where annual Chl degradation amounts to an estimated 1000 million tons on Earth (Hendry et al., 1987). The question has, therefore, been asked repeatedly: “Are PBs not more than only degradation products?” and “Do they have physiological effects in the plants, or else, in the living nature?” (Kräutler, 2016). To date, biological activities of the abundant PBs are hardly explored. However, a striking case for the specific use of Chl-derived linear tetrapyrroles in marine organisms was discovered in the late 1980s (Nakamura, Kishi, Shimomura, Morse, & Hastings, 1989; Nakamura, Musicki, Kishi, & Shimomura, 1988), when it was shown that such bilin-type compounds are produced in different bioluminescing dinoflagellate species, and used as luciferins. Structurally these luciferins were considered to be formed through a remarkable ring opening reaction in the ‘Western’ position of a Chl macrocycle (Topalov & Kishi, 2001), but their biosynthesis still remains to be clarified.

Several fields of research are attractive to address the quest for biological roles of the PBs. Specifically, plant biological and microbiological investigations concerned with potential functions of PBs in higher plants and other photosynthetic organisms would be of interest, possibly generating a range of agrotechnological and horticultural applications. Furthermore, PBs are part of our nutrition and may have metabolic roles in humans and higher animals. This recently acquired knowledge also calls for interest in physiological, pharmacological and biomedical investigations.

In summary, the biology of Chl catabolism and the potential physiological roles of Chl degradation products still harbor many topical questions. It will be interesting to learn more about enzymes that catalyze the respective phyllobilin-modifying reactions, about intracellular and other transport systems for PBs in higher plants, as well as the regulatory networks that control local and general onset and degree of Chl breakdown in response to external and internal signals. The further fate of the ‘late’ PBs and their still unknown physiological roles in higher plants are, likewise, topics that invite further studies.

Table 1. Structures of natural fluorescent 1-formyl-19-oxobilin type (type-I) phyllobilins (FCCs): the labels R^1 to R^4 refer to the generalized formula of FCCs, as shown in Scheme 3.

#[a]	R^1	R^2	R^3	R^4	C16[b]	provisional names[c]	references
2	H	CH_3	H	$CH=CH_2$	n	*Bn*-FCC-2 *(p*FCC*)*	(Mühlecker et al., 1997)
***epi*-2**	H	CH_3	H	$CH=CH_2$	epi	*Ca*-FCC-2 *(epi-p*FCC*)*	(Mühlecker et al., 2000)
5	H	H	H	$CH=CH_2$	n	*At*-FCC-2	(Pružinská et al., 2005)
4	OH	H	H	$CH=CH_2$	n	*At*-FCC-1	(Pružinská et al., 2005)
***epi*-3**	OH	CH_3	H	$CH=CH_2$	epi	*Mc*-FCC-62	(Moser et al., 2012)
12	O-Glc [d]	CH_3	H	$CH=CH_2$	n	*At*-FCC-40	(Christ et al., 2012)
11	OH	CH_3	CH_3 [e]	$CH=CH_2$	epi	*Mc*-FCC-62	(Vergeiner et al., 2013)
9a	OH	CH_3	6‘-βGlc	$CH=CH_2$	epi	*Ma*-FCC-64	(Vergeiner et al., 2013)
9b	OH	CH_3	6‘-βGlc	$CH=CH_2$	epi	*Ma*-FCC-63	(Vergeiner et al., 2013)
6	OH	CH_3	4‘-daucyl [f]	$CH=CH_2$	epi	*Mc*-FCC-56	(Moser et al., 2008a)
***iso*-6**	OH	CH_3	4‘-daucyl [g]	$CH=CH_2$	epi	*Mc*-FCC-53	(Moser et al., 2008a)
7	O–Glc [d]	CH_3	5‘-daucyl [f]	$CH=CH_2$	epi	*Mc*-FCC-49	(Moser et al., 2009)
***iso*-7**	O–Glc [d]	CH_3	4‘-daucyl [g]	$CH=CH_2$	epi	*Mc*-FCC-46	(Moser et al., 2009)
8	OH	CH_3	[h]	$CH=CH_2$	epi	*Ma*-FCC-61	(Banala et al., 2010)
10	OH	CH_3	[i]	$CH=CH_2$	n	*Sw*-FCC-62	(Kräutler et al., 2010)
13	O–Glc* [j]	CH_3	6‘-Glc* [j]	$CH=CH_2$	epi	*Vv*-FCC-55,	(Erhart et al., 2018a)

[a] compound-number; [b] relative configuration at C16: n = ‘normal’, i.e. derived from *p*FCC (**2**); epi = ‘epimeric’, i.e. derived from *epi-p*FCC (***epi*-2**); [c] *Bn*-FCC-2 from oilseed rape (*Brassica napus*);(Mühlecker et al., 1997) *Ca*-FCC-2 from sweet pepper (*Capsicum annuum*);(Mühlecker et al., 2000) *At*-FCCs from *Arabidopsis thaliana*);(Pružinská et al., 2005) *Mc*-FCCs from banana peels (*Musa acuminata*, Cavendish cultivar) (Moser et al., 2008a; Moser et al., 2009; Moser et al., 2012)); *Ma*-FCCs from banana leaves (*Musa acuminata*, Cavendish cultivar) (Banala et al., 2010); *Sw*-FCC-62 from peace lily (*Spathiphyllum wallisii*); (Kräutler et al., 2010) *Vv*-FCC-55 from grapevine (*Vitis vinifera*) (Erhart et al., 2018a); [d] Glc = 1’*β*-D-glucopyranosyl; [e] likely to be an artefact, from methanolysis of 'persistent' FCC-daucyl-esters, such as *Mc*-FCC-56 and *Mc*-FCC-53; [f] bound at daucyl 4’-OH; [g] bound at daucyl 5’-OH; (Moser et al., 2012) [h] R^4 = glyceryl-di-galactosyl (Banala et al., 2010); [i] R^4 = dihydroxyphenylethyl-glucosyl (Kräutler et al., 2010); [j] Glc* = twice attached as 1’*β*,6’-D-glycopyranosyl moiety (Erhart et al., 2018a).

Table 2: Structures of natural nonfluorescent type-I Chl catabolites (NCCs): the labels **R[1]** to **R[4]** refer to the generalized formula of type-I phyllobilanes, atom numbering shown in Scheme 6.

# [a]	R[1] [b]	R[2]	R[3]	R[4]	C16 [c]	provisional name [d]	Ref.
27	H	H	H	$CH=CH_2$	n	*At*-NCC-5 [e],*Bo*-NCC-2	(Pružinská et al., 2005; Roiser et al., 2015)
***epi*-27**	H	H	H	$CH=CH_2$	epi	*Oe*-NCC-4 [e]	(Vergara-Dominguez et al., 2016)
28	H	H	H	$CH=CH_2$	n	*At*-NCC-3 [f]	(Müller et al., 2006)
19	H	CH_3	H	$CH=CH_2$	n	syn [g]	(Oberhuber et al., 2008)
***epi*-19**	H	CH_3	H	$CH=CH_2$	epi	*Cj*-NCC-2	(Oberhuber et al., 2003)
29	OH	H	H	$CH=CH_2$	n	*Bn*-NCC-3	(Mühlecker & Kräutler, 1996)
***epi*-29**	OH	H	H	$CH=CH_2$	epi	*So*-NCC-3	(Berghold et al., 2002)
30	OH	H	H	$CH(OH)-CH_2OH$	epi	*So*-NCC-1	(Berghold et al., 2002)
1	OH	CH_3	H	$CH(OH)-CH_2OH$	n	*Hv*-NCC-1	(Kräutler et al., 1991)
***epi*-1**	OH	CH_3	H	$CH(OH)-CH_2OH$	epi	*So*-NCC-2	(Oberhuber, Berghold, Mühlecker, Hörtensteiner, & Kräutler, 2001)
26	OH	CH_3	H	$CH=CH_2$	n	*Sw*-NCC-58	(Kräutler et al., 2010)
***epi*-26**	OH	CH_3	H	$CH=CH_2$	epi	*Cj*-NCC-1	(Curty & Engel, 1996)
20	O-Glc	H	H	$CH=CH_2$	n	*Bn*-NCC-2	(Mühlecker & Kräutler, 1996)
31	O-Glc	CH_3	H	$CH=CH_2$	n	*At*-NCC-4 [e]	(Pružinská et al., 2005)
32	O-Glc	H	H	$CH(OH)-CH_2OH$	epi?	*Co*-NCC-2 [e]	(Rios et al., 2014a)
33	O-Glc	CH_3	H	$CH(OH)-CH_2OH$	epi	*Zm*-NCC-1	(Berghold et al., 2006)
22	O-Glc	CH_3	H	$CH(OH)CH_2$-O-Glc [h]	epi	*Pd*-NCC-32	(Erhart et al., 2016)
34	O-(6'-OMal)Glc	CH_3	H	$CH=CH_2$	epi	*Nr*-NCC-1	(Berghold et al., 2004)
35	O-Mal	H	H	$CH=CH_2$	n	*Bn*-NCC-1	(Mühlecker et al., 1993)
36	O-Mal	CH_3	H	$CH=CH_2$	epi	*Ej*-NCC-2 [e]	(Rios et al., 2014b)
23	OH	CH_3	[i]	$CH=CH_2$	epi	*Mc*-NCC-58	(Moser et al., 2012)
24	OH	CH_3	[j]	$CH=CH_2$	epi	*Mc*-NCC-55	(Moser et al., 2012)
25	O-Glc [k]	CH_3	6'-βGlc [k]	$CH=CH_2$	epi	*Ug*-NCC-53	(Scherl et al., 2016)
21	OH	-- [l]	H	$CH=CH_2$	epi[h]	*py*NCC (syn [g])	(Li et al., 2018)

[a] Compound-number; [b] abbreviations: Mal = malonyl; Glc = 1'β-D-glucopyranosyl; [c] configuration at C16 from correlation with NCCs derived from *p*FCC (**2**) (n = 'normal') or from *epi-p*FCC (***epi*-2**) (epi = 'epimeric'), the

absolute configuration at C16 is still unknown; [d] *Hv*-NCC-1 from barley (*Hordeum vulgare*);(Kräutler et al., 1992; Kräutler et al., 1991) *So*-NCCs from spinach (*Spinacia oleracea*);(Berghold et al., 2002; Oberhuber et al., 2001) *Cj*-NCCs from Katsura tree, (*Cercidiphyllum japonicum*);(Curty & Engel, 1996) *Sw*-NCC-58 from peace lily (*Spathiphyllum wallisii*);(Kräutler et al., 2010) *Pc*-NCCs from pear (*Pyrus communis*);(Müller et al., 2007) *Md*-NCCs from apple (*Malus domestica*)(Müller et al., 2007), *At*-NCCs (from *Arabidopsis thaliana*;(Müller et al., 2006; Pružinská et al., 2005), *Nr*-NCCs from tobacco (*Nicotiana rustica*);(Berghold et al., 2004) *Zm*-NCCs from maize (*Zea mays*);(Berghold et al., 2006) *Bn*-NCCs from oilseed rape (*Brassica napus*);(Mühlecker & Kräutler, 1996; Mühlecker et al., 1993) *Ej*-NCC from Loquat Fruits (*Eriobotrya japonica*) (Rios et al., 2014b); and *Mc*-NCCs from banana peels (*Musa acuminata*, Cavendish cultivar) (Moser et al., 2012); *Pd*-NCC from plum tree (*Prunus x domestica*) (Erhart et al., 2016); *Ug*-NCC from wych elm (*Ulmus glabra*) (Scherl et al., 2016); [e] identified by UV/Vis and MS; [f] At-NCC-3 carries a HO-CH_2-group at C2 (Müller et al., 2006). [g] from partial synthesis (Li et al., 2018; Oberhuber et al., 2003); [h] Glc = 1'β-D-glucopyranosyl; [i] R^4 = daucyl unit and R-configuration at C10; [j] R^4 = daucyl unit and S-configuration at C10 (as derived from CD-spectra (Moser et al., 2012)); [k] 1',6'-glycopyranosyl bridge attached at O^3 and $O12^4$ (Scherl et al., 2016); [l] unsubstituted H_2C8^2 (Li et al., 2018).

Table 3. Structures of natural dioxobilin-type nonfluorescent Chl catabolites (DNCCs) and of related nonfluorescent dioxobilin-type Chl catabolites (NDCCs): the labels R^1, R^2 and R^4 refer to the generalized constitutional formula of type-II phyllobilanes (see Scheme 7).

a) natural dioxobilin-type nonfluorescent Chl catabolites (DNCCs)

# [a]	R^1	R^2	R^4	C16 [b]	provisional names [c]	references
45	H	H	$CH=CH_2$	n	*At*-DNCC-45 [d]	(Süssenbacher et al., 2015b)
***iso*-45**	H	H	$CH=CH_2$	n	*At*-DNCC-48 [d]	(Süssenbacher et al., 2015b)
16	OH	H	$CH=CH_2$	n	*At*-NDCC-1, *At*-DNCC-33	(Christ et al., 2013; Süssenbacher et al., 2015a)
40	OH	H	$CH=CH_2$	epi	*Hvir*-UNCC [e],*Vv*-DNCC-51	(Djapic, Pavlovic, Arsovski, & Vujic, 2009; Erhart et al., 2018a)
46	OH	CH_3	$CH=CH_2$	n	At_{mes16}-DNCC-38	(Süssenbacher et al., 2014)
37	OH	CH_3	$CH(OH)-CH_2OH$	n	*Hv*-DNCC-a [d,f]	(Losey & Engel, 2001)
38	OH	CH_3	$CH(OH)-CH_2OH$	n	*Hv*-DNCC-b [d,f]	(Losey & Engel, 2001)
39	OH	CH_3	$CH(OH)-CH_2OH$	epi	*Ap*-DNCC	(Müller et al., 2011)

b) nonfluorescent dioxobilin-type Chl catabolites (classified as NDCCs originally (Christ et al., 2013; Süssenbacher et al., 2014) that carry a new CH_2OH substituent, listed as HM-DNCCs and HM-*iso*-DNCCs (see Scheme 7)

# [a]	R^1	R^2	R^4	C16 [b]	provisional names [c]	references
41	H	H	$CH_2=CH_2$	n	*At*-4HM-DNCC-41 [g]	(Süssenbacher et al., 2015b)
43	H	H	$CH=CH_2$	n	*At*-2HM-*iso* DNCC-43 [h]	(Süssenbacher et al., 2015b)
42	H	CH_3	$CH=CH_2$	n	At_{mes16}-4HM-DNCC-44 [g]	(Süssenbacher et al., 2014)
44	H	CH_3	$CH_2=CH_2$	n	At_{mes16}-2HM-*iso*-DNCC-46 [h]	(Süssenbacher et al., 2014)

[a] compound number; [b] configuration at C16: n = 'normal', derived from *p*FCC; epi = 'epimeric', derived from *epi*-*p*FCC; [c] for specific provisional names see references: e.g. *Ap*-DNCC (from *Acer platanoides*); *At*-PBs (from *Arabidopsis thaliana*); At_{mes16}-PBs from *mes16* mutant of *Arabidopsis*; *Hv*-DNCCs from barley (*Hordeum vulgare*); *Vv*-DNCC from grapevine (*Vitis vinifera*); [d] presumed to be C4-stereoisomers pairwise; [e] abbreviation used in the original paper (Djapic et al., 2009); [f] a name was not given in the original paper (Losey & Engel, 2001), adaptation to nomenclature used now; [g] carries an extra CH_2OH unit at C4; [h] is unsaturated between C3 and C4 and carries the additional CH_2OH unit at C2.

References

Abbas, M., Hernandez-Garcia, J., Pollmann, S., Samodelov, S. L., Kolb, M., Friml, J., et al. (2018). Auxin methylation is required for differential growth in Arabidopsis. *Proceedings of the National Academy of Sciences, USA, 115*, 6864-6869.

Abeles, F. B., Dunn, L. J., Morgens, P., Callahan, A., Dinterman, R. E., & Schmidt, J. (1988). Induction of 33-Kd and 60-Kd peroxidases during ethylene-induced senescence of cucumber cotyledons. *Plant Physiology, 87*, 609-615.

Armstead, I., Donnison, I., Aubry, S., Harper, J., Hörtensteiner, S., James, C., et al. (2006). From crop to model to crop: identifying the genetic basis of the staygreen mutation in the *Lolium*/*Festuca* forage and amenity grasses. *New Phytologist, 172*, 592-597.

Aubry, S., Fankhauser, N., Ovinnikov, S., Zienkiewicz, K., Feussner, I., & Hörtensteiner, S. (2018). Pheophorbide *a*, a chlorophyll catabolite may regulate jasmonate signalling during dark-induced senescence in Arabidopsis. *BioRxiv*, 486886.

Azoulay-Shemer, T., Harpaz-Saad, S., Cohen-Peer, R., Mett, A., Spicer, V., Lovat, N., et al. (2011). Dual N- and C-terminal processing of Citrus chlorophyllase precursor within the plastid membranes leads to the mature enzyme. *Plant and Cell Physiology, 52*, 70-83.

Azoulay Shemer, T., Harpaz-Saad, S., Belausov, E., Lovat, N., Krokhin, O., Spicer, V., et al. (2008). *Citrus* chlorophyllase dynamics at ethylene-induced fruit color-break; a study of chlorophyllase expression, post-translational processing kinetics and *in-situ* intracellular localization. *Plant Physiology, 148*, 108-118.

Balsera, M., Soll, J., & Buchanan, B. B. (2010). Redox extends its regulatory reach to chloroplast protein import. *Trends in Plant Science, 15*, 515-521.

Banala, S., Moser, S., Müller, T., Kreutz, C. R., Holzinger, A., Lütz, C., et al. (2010). Hypermodified fluorescent chlorophyll catabolites: source of blue luminescence in senescent leaves. *Angewandte Chemie International Edition, 49*, 5174-5177.

Barsan, C., Sanchez-Bel, P., Rombaldi, C., Egea, I., Rossignol, M., Kuntz, M., et al. (2010). Characteristics of the tomato chromoplast revealed by proteomic analysis. *Journal of Experimental Botany, 61*, 2413-2431.

Barsan, C., Zouine, M., Maza, E., Bian, W., Egea, I., Rossignol, M., et al. (2012). Proteomic analysis of chloroplast-to-chromoplast transition in tomato reveals metabolic shifts coupled with disrupted thylakoid biogenesis machinery and elevated energy-production components. *Plant Physiology, 160*, 708-725.

Bartsch, S., Monnet, J., Selbach, K., Quigley, F., Gray, J., von Wettstein, D., et al. (2008). Three thioredoxin targets in the inner envelope membrane of chloroplasts function in protein import and chlorophyll metabolism. *Proceedings of the National Academy of Sciences, USA, 105*, 4933-4938.

Berghold, J., Breuker, K., Oberhuber, M., Hörtensteiner, S., & Kräutler, B. (2002). Chlorophyll breakdown in spinach: on the structure of five nonfluorescent chlorophyll catabolites. *Photosynthesis Research, 74*, 109-119.

Berghold, J., Eichmüller, C., Hörtensteiner, S., & Kräutler, B. (2004). Chlorophyll breakdown in tobacco: on the structure of two nonfluorescent chlorophyll catabolites. *Chemistry & Biodiversity, 1*, 657-668.

Berghold, J., Müller, T., Ulrich, M., Hörtensteiner, S., & Kräutler, B. (2006). Chlorophyll breakdown in maize: on the structure of two nonfluorescent chlorophyll catabolites. *Monatshefte für Chemie, 137*, 751-763.

Biswal, U. C., & Biswal, B. (1984). Photocontrol of leaf senescence. *Photochemistry and Photobiology, 39*, 875-879.

Bleecker, A. B., Estelle, M. A., Somerville, C., & Kende, H. (1988). Insensitivity to ethylene conferred by a dominant mutation in *Arabidopsis thaliana*. *Science, 241*, 1086-1089.

Boij, P., Patel, R., Garcia, C., Jarvis, P., & Aronsson, H. (2009). In vivo studies on the roles of Tic55-related proteins in chloroplast protein import in *Arabidopsis thaliana*. *Molecular Plant, 2*, 1397-1409.

Bortlik, K.-H., Peisker, C., & Matile, P. (1990). A novel type of chlorophyll catabolite in senescent barley leaves. *Journal of Plant Physiology, 136*, 161-165.

Breeze, E., Harrison, E., McHattie, S., Hughes, L., Hickman, R., Hill, C., et al. (2011). High-resolution temporal profiling of transcripts during *Arabidopsis* leaf senescence reveals a distinct chronology of processes and regulation. *The Plant Cell, 23*, 873-894.

Brown, S. B., Houghton, J. D., & Hendry, G. A. F. (1991). Chlorophyll breakdown. In H. Scheer (Ed.), *Chlorophylls* (pp. 465-489). Boca Raton: CRC Press.

Büchert, A. M., Civello, P. M., & Martínez, G. A. (2011). Chlorophyllase versus pheophytinase as candidates for chlorophyll dephytilation during senescence of broccoli. *Journal of Plant Physiology, 168*, 337-343.

Calibe, A., Grimm, R., Kaiser, G., Lübeck, J., Soll, J., & Heins, L. (1997). The chloroplastic protein import machinery contains a Rieske-type iron-sulfur cluster and a mononuclear iron-binding protein. *The EMBO Journal, 16*, 7342-7350.

Chao, Q. M., Rothenberg, M., Solano, R., Roman, G., Terzaghi, W., & Ecker, J. R. (1997). Activation of the ethylene gas response pathway in Arabidopsis by the nuclear protein ETHYLENE-INSENSITIVE3 and related proteins. *Cell, 89*, 1133-1144.

Cheng, Y. D., & Guan, J. F. (2014). Involvement of pheophytinase in ethylene-mediated chlorophyll degradation in the peel of harvested 'Yali' pear. *Journal of Plant Growth Regulation, 33*, 364-372.

Christ, B., Hauenstein, M., & Hörtensteiner, S. (2016). A liquid chromatography-mass spectrometry platform for the analysis of phyllobilins, the major degradation products of chlorophyll in *Arabidopsis thaliana*. *The Plant Journal, 88*, 505-518.

Christ, B., Schelbert, S., Aubry, S., Süssenbacher, I., Müller, T., Kräutler, B., et al. (2012). MES16, a member of the methylesterase protein family, specifically demethylates fluorescent chlorophyll catabolites during chlorophyll breakdown in Arabidopsis. *Plant Physiology, 158*, 628-641.

Christ, B., Süssenbacher, I., Moser, S., Bichsel, N., Egert, A., Müller, T., et al. (2013). Cytochrome P450 CYP89A9 is involved in the formation of major chlorophyll catabolites during leaf senescence in *Arabidopsis*. *The Plant Cell, 25*, 1868-1880.

Curty, C., & Engel, N. (1996). Detection, isolation and structure elucidation of a chlorophyll *a* catabolite from autumnal senescent leaves of *Cercidiphyllum japonicum*. *Phytochemistry, 42*, 1531-1536.

Curty, C., Engel, N., & Gossauer, A. (1995). Evidence for a monooxygenase-catalyzed primary process in the catabolism of chlorophyll. *FEBS Letters, 364*, 41-44.

Das, A., Christ, B., & Hörtensteiner, S. (2018). Characterization of the pheophorbide *a* oxygenase/phyllobilin pathway of chlorophyll breakdown in grasses. *Planta, 248*, 875-892.

Delmas, F., Sankaranarayanan, S., Deb, S., Widdup, E., Bournonville, C., Bollier, N., et al. (2013). ABI3 controls embryo degreening through Mendel's I locus. *Proceedings of the National Academy of Sciences, USA, 110*, E3888-E3894.

Djapic, N., Pavlovic, M., Arsovski, S., & Vujic, G. (2009). Chlorophyll biodegradation product from *Hamamelis virginiana* autumnal leaves. *Revista De Chimie, 60*, 398-402.

Düggelin, T., Schellenberg, M., Bortlik, K.-H., & Matile, P. (1988). Vacuolar location of lipofuscin-and proline-like compounds in senescent barley leaves. *Journal of Plant Physiology, 133*, 492-497.

Engel, N., Curty, C., & Gossauer, A. (1996). Chlorophyll catabolism in *Chlorella protothecoides*. 8. Facts and artefacts. *Plant Physiology and Biochemistry, 34*, 77-83.

Engel, N., Gossauer, A., Gruber, K., & Kratky, C. (1993). X-ray molecular structure of a red bilin derivative from *Chlorella protothecoides*. *Helvetica Chimica Acta, 76*, 1-3.

Erhart, T., Mittelberger, C., Liu, X., Podewitz, M., Li, C., Scherzer, G., et al. (2018a). Novel types of hypermodified fluorescent phyllobilins from breakdown of chlorophyll in senescent leaves of grapevine (*Vitis vinifera*). *Chemistry - A European Journal, 24*, 17268-17279.

Erhart, T., Mittelberger, C., Vergeiner, C., Scherzer, G., Holzner, B., Robatscher, P., et al. (2016). Chlorophyll catabolites in senescent leaves of the plum tree (*Prunus domestica*). *Chemistry & Biodiversity, 13*, 1441-1453.

Erhart, T., Vergeiner, S., Kreutz, C., Kräutler, B., & Müller, T. (2018b). Chlorophyll breakdown in a fern - discovery of phyllobilin isomers with a rearranged carbon skeleton. *Angewandte Chemie International Edition, 57*, 14937-14941.

Falk, H. (1989). *Chemistry of Linear Oligopyrroles and Bile Pigments*. Wien: Springer.

Falk, H., Hoornaert, G., Isenring, H. P., & Eschenmoser, A. (1975). Enol derivatives in chlorophyll series - preparation of 13^2,17^3-cyclopheophorbide enols. *Helvetica Chimica Acta, 58*, 2347-2357.

Fang, C., Li, C. C., Li, W. Y., Wang, Z., Zhou, Z. K., Shen, Y. T., et al. (2014). Concerted evolution of D1 and D2 to regulate chlorophyll degradation in soybean. *The Plant Journal, 77*, 700-712.

Frankenberg, N., Mukougawa, K., Kohchi, T., & Lagarias, J. C. (2001). Functional genomic analysis of the HY2 family of ferredoxin-dependent bilin reductases from oxygenic photosynthetic organisms. *The Plant Cell, 13*, 965-978.

Gao, C. F., Wang, Y., Shen, Y., Yan, D., He, X., Dai, J. B., et al. (2014). Oil accumulation mechanisms of the oleaginous microalga *Chlorella protothecoides* revealed through its genome, transcriptomes, and proteomes. *BMC Genomics, 15*.

Gepstein, S., Sabehi, G., Carp, M. J., Hajouj, T., Nesher, M. F. O., Yariv, I., et al. (2003). Large-scale identification of leaf senescence-associated genes. *The Plant Journal, 36*, 629-642.

Gepstein, S., & Thimann, K. V. (1980). Changes in the abscisic-acid content of oat leaves during senescence. *Proceedings of the National Academy of Sciences, USA, 77*, 2050-2053.

Gomez, M. D., Vera-Sirera, F., & Perez-Amador, M. A. (2014). Molecular programme of senescence in dry and fleshy fruits. *Journal of Experimental Botany, 65*, 4515-4526.

Gray, J., Wardzala, E., Yang, M., Reinbothe, S., Haller, S., & Pauli, F. (2004). A small family of LLS1-related non-heme oxygenases in plants with an origin amongst oxygenic photosynthesizers. *Plant Molecular Biology, 54*, 39-54.

Greenberg, J. T., & Ausubel, F. M. (1993). *Arabidopsis* mutants compromised for the control of cellular damage during pathogenesis and aging. *The Plant Journal, 4*, 327-341.

Greenberg, J. T., Guo, A., Klessig, D. F., & Ausubel, F. M. (1994). Programmed cell death in plants: a pathogen-triggered response activated coordinately with multiple defense functions. *Cell, 77*, 551-563.

Guo, Y. F., & Gan, S. S. (2012). Convergence and divergence in gene expression profiles induced by leaf senescence and 27 senescence-promoting hormonal, pathological and environmental stress treatments. *Plant, Cell & Environment, 35*, 644-655.

Guyer, L., Salinger, K., Krügel, U., & Hörtensteiner, S. (2018). Catalytic and structural properties of pheophytinase, the phytol esterase involved in chlorophyll breakdown. *Journal of Experimental Botany, 69*, 879–889.

Guyer, L., Schelbert Hofstetter, S., Christ, B., Silverstre Lira, B., Rossi, M., & Hörtensteiner, S. (2014). Different mechanisms are responsible for chlorophyll dephytylation during fruit ripening and leaf senescence in tomato. *Plant Physiology, 166*, 44-56.

Hauenstein, M., Christ, B., Das, A., Aubry, S., & Hörtensteiner, S. (2016). A role for TIC55 as a hydroxylase of phyllobilins, the products of chlorophyll breakdown during plant senescence. *The Plant Cell, 28*, 2510-2527.

He, Y. H., Fukushige, H., Hildebrand, D. F., & Gan, S. S. (2002). Evidence supporting a role of jasmonic acid in Arabidopsis leaf senescence. *Plant Physiology, 128*, 876-884.

Hendry, G. A. F., Houghton, J. D., & Brown, S. B. (1987). The degradation of chlorophyll - A biological enigma. *New Phytologist, 107*, 255-302.

Hinder, B., Schellenberg, M., Rodoni, S., Ginsburg, S., Vogt, E., Martinoia, E., et al. (1996). How plants dispose of chlorophyll catabolites. Directly energized uptake of tetrapyrrolic breakdown products into isolated vacuoles. *The Journal of Biological Chemistry, 271*, 27233-27236.

Hirashima, M., Tanaka, R., & Tanaka, A. (2009). Light-independent cell death induced by accumulation of pheophorbide *a* in *Arabidopsis thaliana*. *Plant and Cell Physiology, 50*, 719-729.

Horie, Y., Ito, H., Kusaba, M., Tanaka, R., & Tanaka, A. (2009). Participation of chlorophyll *b* reductase in the initial step of the degradation of light-harvesting chlorophyll *a*/*b*-protein complexes in *Arabidopsis*. *The Journal of Biological Chemistry, 284*, 17449-17456.

Hörtensteiner, S. (1998). NCC malonyltransferase catalyses the final step of chlorophyll breakdown in rape (*Brassica napus*). *Phytochemistry, 49*, 953-956.

Hörtensteiner, S. (2004). The loss of green color during chlorophyll degradation - a prerequisite to prevent cell death? *Planta, 219*, 191-194.

Hörtensteiner, S. (2006). Chlorophyll degradation during senescence. *Annual Review of Plant Biology, 57*, 55-77.

Hörtensteiner, S. (2009). Stay-green regulates chlorophyll and chlorophyll-binding protein degradation during senescence. *Trends in Plant Science, 14*, 155-162.

Hörtensteiner, S. (2013). Update on the biochemistry of chlorophyll breakdown. *Plant Molecular Biology, 82*, 505-517.

Hörtensteiner, S., & Kräutler, B. (2011). Chlorophyll breakdown in higher plants. *Biochimica et Biophysica Acta, 1807*, 977-988.

Hörtensteiner, S., Rodoni, S., Schellenberg, M., Vicentini, F., Nandi, O. I., Qiu, Y.-L., et al. (2000). Evolution of chlorophyll degradation: the significance of RCC reductase. *Plant Biology, 2*, 63-67.

Hörtensteiner, S., Vicentini, F., & Matile, P. (1995). Chlorophyll breakdown in senescent cotyledons of rape, *Brassica napus* L.: enzymatic cleavage of phaeophorbide *a in vitro*. *New Phytologist, 129*, 237-246.

Hörtensteiner, S., Wüthrich, K. L., Matile, P., Ongania, K.-H., & Kräutler, B. (1998). The key step in chlorophyll breakdown in higher plants. Cleavage of pheophorbide *a* macrocycle by a monooxygenase. *The Journal of Biological Chemistry, 273*, 15335-15339.

Hynninen, P. H., Kaartinen, V., & Kolehmainen, E. (2010). Horseradish peroxidase-catalyzed oxidation of chlorophyll *a* with hydrogen peroxide. Characterization of the products and mechanism of the reaction. *Biochimica et Biophysica Acta, 1797*, 531-542.

Inada, N., Sakai, A., Kuroiwa, H., & Kuroiwa, T. (1998). Three-dimensional analysis of the senescence program in rice (Oryza sativa L.) coleoptiles. Investigations of tissues and cells by fluorescence microscopy. *Planta, 205*, 153-164.

Jiang, H., Li, M., Liang, N., Yan, H., Wei, Y., Xu, X., et al. (2007). Molecular cloning and function analysis of the *stay green* gene in rice. *The Plant Journal, 52*, 197-209.

Jiang, Y. J., Liang, G., Yang, S. Z., & Yu, D. Q. (2014). Arabidopsis WRKY57 functions as a node of convergence for jasmonic acid- and auxin-mediated signaling in jasmonic acid-induced leaf senescence. *The Plant Cell, 26*, 230-245.

Jockusch, S., Turro, N. J., Banala, S., & Kräutler, B. (2014). Photochemical studies of a fluorescent chlorophyll catabolite - source of bright blue fluorescence in plant tissue and

efficient sensitizer of singlet oxygen. *Photochemical & Photobiological Sciences, 13*, 407-411.

Johnson-Flanagan, A. M., & Spencer, M. S. (1996). Chlorophyllase and peroxidase activity during degreening of maturing canola (*Brassica napus*) and mustard (*Brassica juncea*) seed. *Physiologia Plantarum, 97*, 353-359.

Kahlau, S., & Bock, R. (2008). Plastid transcriptomics and translatomics of tomato fruit development and chloroplast-to-chromoplast differentiation: Chromoplast gene expression largely serves the production of a single protein. *The Plant Cell, 20*, 856-874.

Kang, J., Park, J., Choi, H., Burla, B., Kretzschmar, T., Lee, Y., et al. (2011). Plant ABC transporters. *The Arabidopsis Book, 9*, e0153.

Kashiyama, Y., & Tamiaki, H. (2014). Risk management by organisms of the phototoxicity of chlorophylls. *Chemistry Letters, 43*, 148-156.

Kashiyama, Y., Yokoyama, A., Kinoshita, Y., Shoji, S., Miyashiya, H., Shiratori, T., et al. (2012). Ubiquity and quantitative significance of detoxification catabolism of chlorophyll associated with protistan herbivory. *Proceedings of the National Academy of Sciences, USA, 109*, 17328-17335.

Kashiyama, Y., Yokoyama, A., Shiratori, T., Inouye, I., Kinoshita, Y., Mizoguchi, T., et al. (2013). 13^2,17^3-Cyclopheophorbide *b* enol as a catabolite of chlorophyll *b* in phycophagy by protists. *FEBS Letters, 587*, 2578-2583.

Kräutler, B. (2014). Phyllobilins - the abundant bilin-type tetrapyrrolic catabolites of the green plant pigment chlorophyll. *Chemical Society Reviews, 43*, 6227-6238.

Kräutler, B. (2016). Breakdown of chlorophyll in higher plants - Phyllobilins as abundant, yet hardly visible signs of ripening, senescence, and cell death. *Angewandte Chemie International Edition, 55*, 4882-4907.

Kräutler, B. (2019). How chemistry has helped to decipher a striking biological enigma. *Synlett, 30*, 263-274.

Kräutler, B., Banala, S., Moser, S., Vergeiner, C., Müller, T., Lütz, C., et al. (2010). A novel blue fluorescent chlorophyll catabolite accumulates in senescent leaves of the peace lily and indicates a divergent path of chlorophyll breakdown. *FEBS Letters, 584*, 4215-4221.

Kräutler, B., & Hörtensteiner, S. (2014). Chlorophyll breakdown: chemistry, biochemistry and biology. In G. C. Ferreira, K. M. Kadish, K. M. Smith, & R. Guilard (Eds.), *Handbook*

of Porphyrin Science - Chlorophyll, Photosynthesis and Bio-inspired Energy (Vol. 28, pp. 117-185). Singapore: World Scientific Publishing.

Kräutler, B., Jaun, B., Amrein, W., Bortlik, K., Schellenberg, M., & Matile, P. (1992). Breakdown of chlorophyll: Constitution of a secoporphinoid chlorophyll catabolite isolated from senescent barley leaves. *Plant Physiology and Biochemistry, 30*, 333-346.

Kräutler, B., Jaun, B., Bortlik, K.-H., Schellenberg, M., & Matile, P. (1991). On the enigma of chlorophyll degradation: the constitution of a secoporphinoid catabolite. *Angewandte Chemie International Edition, 30*, 1315-1318.

Kräutler, B., & Matile, P. (1999). Solving the riddle of chlorophyll breakdown. *Accounts of Chemical Research, 32*, 35-43.

Kräutler, B., Mühlecker, W., Anderl, M., & Gerlach, B. (1997). Breakdown of chlorophyll: partial synthesis of a putative intermediary catabolite. *Helvetica Chimica Acta, 80*, 1355-1362.

Krupinska, K., Biswal, U. C., & Biswal, B. (2013). The dynamic role of chloroplasts in integrating plant growth and development. In B. Biswal, K. Krupinska, & U. C. Biswal (Eds.), *Plastid Development in Leaves during Growth and Senescence* (Vol. 36, pp. 3-16). Dordrecht, The Netherlands: Pringer.

Kuai, B., Chen, J., & Hörtensteiner, S. (2018). The biochemistry and molecular biology of chlorophyll breakdown. *Journal of Experimental Botany, 69*, 751–767.

Kusaba, M., Ito, H., Morita, R., Iida, S., Sato, Y., Fujimoto, M., et al. (2007). Rice NON-YELLOW COLORING1 is involved in light-harvesting complex II and grana degradation during leaf senescence. *The Plant Cell, 19*, 1362-1375.

Li, C. J., Erhart, T., Liu, X. J., & Kräutler, B. (2019). Yellow dioxobilin-type tetrapyrroles from chlorophyll breakdown in higher plants - A new class of colored phyllobilins. *Chemistry - A European Journal, in press. doi: 10.1002/chem.201806038*.

Li, C. J., & Kräutler, B. (2019). A pink colored dioxobilin-type phyllobilin from breakdown of chlorophyll. *Monatshefte für Chemie, in press. doi: 10.1007/s00706-019-02396-5*.

Li, C. J., Ulrich, M., Liu, X. J., Wurst, K., Müller, T., & Kräutler, B. (2014). Blue transition metal complexes of a natural bilin-type chlorophyll catabolite. *Chemical Science, 5*, 3388-3395.

Li, C. J., Wurst, K., Berghold, J., Podewitz, M., Liedl, K. R., & Kräutler, B. (2018). Pyro-phyllobilins: elusive chlorophyll catabolites lacking a critical carboxylate function of the natural chlorophylls. *Chemistry - A European Journal, 24*, 2987-2998.

Li, C. J., Wurst, K., Jockusch, S., Gruber, K., Podewitz, M., Liedl, K. R., et al. (2016). Chlorophyll-derived yellow phyllobilins of higher plants as medium-responsive chiral photoswitches. *Angewandte Chemie International Edition, 55*, 15760-15765.

Li, H. M., & Pu, H. (2016). Crystal structure of methylesterase family member 16 (MES16) from *Arabidopsis thaliana*. *Biochemical and Biophysical Research Communications, 474*, 226-231.

Li, L., Ban, Z., Limwachiranon, J., & Luo, Z. (2017). Proteomic studies on fruit ripening and senescence. *Critical Reviews in Plant Sciences, 36*, 116-127.

Li, Z. P., Wu, S. X., Chen, J. Y., Wang, X. Y., Gao, J., Ren, G. D., et al. (2017). NYEs/SGRs-mediated chlorophyll degradation is critical for detoxification during seed maturation in Arabidopsis. *The Plant Journal, 92*, 650-661.

Liebsch, D., & Keech, O. (2016). Dark-induced leaf senescence: new insights into a complex light-dependent regulatory pathway. *New Phytologist, 212*, 563-570.

Lim, P. O., Kim, H. J., & Nam, H. G. (2007). Leaf senescence. *Annual Review of Plant Biology, 58*, 115-136.

Lin, Y. P., Wu, M. C., & Charng, Y. Y. (2016). Identification of a chlorophyll dephytylase involved in chlorophyll turnover in Arabidopsis. *The Plant Cell, 28*, 2974-2990.

Liu, T., Longhurst, A. D., Talavera-Rauh, F., Hokin, S. A., & Barton, M. K. (2016). The Arabidopsis transcription factor ABIG1 relays ABA signaled growth inhibition and drought induced senescence. *eLife, 5*, e13768.

Losey, F. G., & Engel, N. (2001). Isolation and characterization of a urobilinogenoidic chlorophyll catabolite from *Hordeum vulgare* L. *The Journal of Biological Chemistry, 276*, 27233-27236.

Lu, Y.-P., Li, Z.-S., Drozdowicz, Y.-M., Hörtensteiner, S., Martinoia, E., & Rea, P. A. (1998). AtMRP2, an Arabidopsis ATP binding cassette transporter able to transport glutathione *S*-conjugates and chlorophyll catabolites: functional comparisons with AtMRP1. *The Plant Cell, 10*, 267-282.

Mach, J. M., Castillo, A. R., Hoogstraten, R., & Greenberg, J. T. (2001). The *Arabidopsis*-accelerated cell death gene *ACD2* encodes red chlorophyll catabolite reductase and suppresses the spread of disease symptoms. *Proceedings of the National Academy of Sciences, USA, 98*, 771-776.

Matile, P. (1980). Catabolism of chlorophyll: involvement of peroxidase? *Zeitschrift für Pflanzenphysiologie, 99*, 457-478.

Matile, P. (1987). Seneszenz bei Pflanzen und ihre Bedeutung für den Stickstoffhaushalt. *Chimia, 41*, 376-381.

Matile, P. (2000). Biochemistry of Indian summer: physiology of autumnal leaf coloration. *Experimental Gerontology, 35*, 145-158.

Matile, P., Ginsburg, S., Schellenberg, M., & Thomas, H. (1987). Catabolites of chlorophyll in senescent leaves. *Journal of Plant Physiology, 129*, 219-228.

Matile, P., Ginsburg, S., Schellenberg, M., & Thomas, H. (1988). Catabolites of chlorophyll in senescing barley leaves are localized in the vacuoles of mesophyll cells. *Proceedings of the National Academy of Sciences, USA, 85*, 9529-9532.

Matile, P., Hörtensteiner, S., & Thomas, H. (1999). Chlorophyll degradation. *Annual Review of Plant Physiology and Plant Molecular Biology, 50*, 67-95.

Matile, P., Hörtensteiner, S., Thomas, H., & Kräutler, B. (1996). Chlorophyll breakdown in senescent leaves. *Plant Physiology, 112*, 1403-1409.

Matile, P., Schellenberg, M., & Peisker, C. (1992). Production and release of a chlorophyll catabolite in isolated senescent chloroplasts. *Planta, 187*, 230-235.

Mecey, C., Hauck, P., Trapp, M., Pumplin, N., Plovanich, A., Yao, J., et al. (2011). A critical role of *STAYGREEN*/Mendel's *I* locus in controlling disease symptom development during *Pseudomonas syringae* pv *tomato* infection of Arabidopsis. *Plant Physiology, 157*, 1965-1974.

Meguro, M., Ito, H., Takabayashi, A., Tanaka, R., & Tanaka, A. (2011). Identification of the 7-hydroxymethyl chlorophyll *a* reductase of the chlorophyll cycle in *Arabidopsis*. *The Plant Cell, 23*, 3442-3453.

Mendel, G. (1866). Versuche über Pflanzenhybriden. *Verhandlungen des naturforschenden Vereines in Brünn, 4*, 3-47.

Mittelberger, C., Yalcinkaya, H., Pichler, C., Gasser, J., Scherzer, G., Erhart, T., et al. (2017). Pathogen-induced leaf chlorosis: products of chlorophyll breakdown found in degreened leaves of Phytoplasma-infected apple (*Malus x domestica* Borkh.) and spricot (*Prunus armeniaca* L.) trees relate to the pheophorbide *a* oxygenase/phyllobilin pathway. *Journal of Agricultural and Food Chemistry, 65*, 2651-2660.

Mizzotti, C., Rotasperti, L., Moretto, M., Tadini, L., Resentini, F., Galliani, B. M., et al. (2018). Time-course transcriptome analysis of Arabidopsis siliques discloses genes essential for fruit development and maturation. *Plant Physiology, 178*, 1249-1268.

Morel, A. (2006). Meeting the challenge of monitoring chlorophyll in the ocean from outer space. In B. Grimm, R. Porra, W. Rüdiger, & H. Scheer (Eds.), *Chlorophylls and*

Bacteriochlorophylls. Biochemistry, Biophysics, Functions and Applications (Vol. 25, pp. 521-534). Dordrecht, The Netherlands: Springer.

Morita, R., Sato, Y., Masuda, Y., Nishimura, M., & Kusaba, M. (2009). Defect in non-yellow coloring 3, an a/b hydrolase-fold family protein, causes a stay-green phenotype during leaf senescence in rice. *The Plant Journal, 59*, 940-952.

Moser, S., Müller, T., Ebert, M. O., Jockusch, S., Turro, N. J., & Kräutler, B. (2008a). Blue luminescence of ripening bananas. *Angewandte Chemie International Edition, 47*, 8954-8957.

Moser, S., Müller, T., Holzinger, A., Lutz, C., Jockusch, S., Turro, N. J., et al. (2009). Fluorescent chlorophyll catabolites in bananas light up blue halos of cell death. *Proceedings of the National Academy of Sciences, USA, 106*, 15538-15543.

Moser, S., Müller, T., Holzinger, A., Lutz, C., & Kräutler, B. (2012). Structures of chlorophyll catabolites in bananas (*Musa acuminata*) reveal a split path of chlorophyll breakdown in a ripening fruit. *Chemistry - A European Journal, 18*, 10873-10885.

Moser, S., Scherzer, G., & Kräutler, B. (2017). On the nature of isomeric nonfluorescent chlorophyll catabolites in leaves and fruit - a study with a ubiquitous phylloleucobilin and its main isomerization product. *Chemistry & Biodiversity, 14*, e1700368.

Moser, S., Ulrich, M., Müller, T., & Kräutler, B. (2008b). A yellow chlorophyll catabolite is a pigment of the fall colours. *Phytochemical & Phytobiological Sciences, 7*, 1577-1581.

Mühlecker, W., & Kräutler, B. (1996). Breakdown of chlorophyll: constitution of nonfluorescing chlorophyll-catabolites from senescent cotyledons of the dicot rape. *Plant Physiology and Biochemistry, 34*, 61-75.

Mühlecker, W., Kräutler, B., Ginsburg, S., & Matile, P. (1993). Breakdown of chlorophyll: A tetrapyrrolic chlorophyll catabolite from senescent rape leaves. *Helvetica Chimica Acta, 76*, 2976-2980.

Mühlecker, W., Kräutler, B., Moser, D., Matile, P., & Hörtensteiner, S. (2000). Breakdown of chlorophyll: a fluorescent chlorophyll catabolite from sweet pepper (*Capsicum annuum*). *Helvetica Chimica Acta, 83*, 278-286.

Mühlecker, W., Ongania, K.-H., Kräutler, B., Matile, P., & Hörtensteiner, S. (1997). Tracking down chlorophyll breakdown in plants: elucidation of the constitution of a 'fluorescent' chlorophyll catabolite. *Angewandte Chemie International Edition, 36*, 401-404.

Müller, T., Moser, S., Ongania, K.-H., Pružinská, A., Hörtensteiner, S., & Kräutler, B. (2006). A divergent path of chlorophyll breakdown in the model plant *Arabidopsis thaliana*. *ChemBioChem, 7*, 40-42.

Müller, T., Rafelsberger, M., Vergeiner, C., & Kräutler, B. (2011). A dioxobilane as product of a divergent path of chlorophyll breakdown in Norway maple. *Angewandte Chemie International Edition, 50*, 10724-10727.

Müller, T., Ulrich, M., Ongania, K. H., & Kräutler, B. (2007). Colorless tetrapyrrolic chlorophyll catabolites found in ripening fruit are effective antioxidants. *Angewandte Chemie International Edition, 46*, 8699-8702.

Mur, L. A. J., Aubry, S., Mondhe, M., Kingston-Smith, A., Gallagher, J., Timms-Taravella, E., et al. (2010). Accumulation of chlorophyll catabolites photosensitizes the hypersensitive response elicited by *Pseudomonas syringae* in Arabidopsis. *New Phytologist, 188*, 161-174.

Nagane, T., Tanaka, A., & Tanaka, R. (2010). Involvement of AtNAP1 in the regulation of chlorophyll degradation in *Arabidopsis thaliana*. *Planta, 231*, 939-949.

Nakajima, S., Ito, H., Tanaka, R., & Tanaka, A. (2012). Chlorophyll *b* reductase plays an essential role in maturation and storability of Arabidopsis seeds. *Plant Physiology, 160*, 261-273.

Nakamura, H., Kishi, Y., Shimomura, O., Morse, D., & Hastings, J. W. (1989). Structure of dinoflagellate luciferin and its enzymatic and nonenzymatic air-oxidation products. *Journal of the American Chemical Society, 111*, 7607-7611.

Nakamura, H., Musicki, B., Kishi, Y., & Shimomura, O. (1988). Structure of the light emitter in krill (*Euphausia pacifica*) bioluminescence. *Journal of the American Chemical Society, 110*, 2683-2685.

Oberhuber, M., Berghold, J., Breuker, K., Hörtensteiner, S., & Kräutler, B. (2003). Breakdown of chlorophyll: a nonenzymatic reaction accounts for the formation of the colorless "nonfluorescent" chlorophyll catabolites. *Proceedings of the National Academy of Sciences, USA, 100*, 6910-6915.

Oberhuber, M., Berghold, J., & Kräutler, B. (2008). Chlorophyll breakdown by a biomimetic route. *Angewandte Chemie International Edition, 47*, 3057-3061.

Oberhuber, M., Berghold, J., Mühlecker, W., Hörtensteiner, S., & Kräutler, B. (2001). Chlorophyll breakdown - on a nonfluorescent chlorophyll catabolite from spinach. *Helvetica Chimica Acta, 84*, 2615-2627.

Park, S.-Y., Yu, J.-W., Park, J.-S., Li, J., Yoo, S.-C., Lee, N.-Y., et al. (2007). The senescence-induced staygreen protein regulates chlorophyll degradation. *The Plant Cell, 19*, 1649-1664.

Pružinská, A., Anders, I., Aubry, S., Schenk, N., Tapernoux-Lüthi, E., Müller, T., et al. (2007). In vivo participation of red chlorophyll catabolite reductase in chlorophyll breakdown. *The Plant Cell, 19*, 369-387.

Pružinská, A., Anders, I., Tanner, G., Roca, M., & Hörtensteiner, S. (2003). Chlorophyll breakdown: pheophorbide *a* oxygenase is a Rieske-type iron-sulfur protein, encoded by the *accelerated cell death 1* gene. *Proceedings of the National Academy of Sciences, USA, 100*, 15259-15264.

Pružinská, A., Tanner, G., Aubry, S., Anders, I., Moser, S., Müller, T., et al. (2005). Chlorophyll breakdown in senescent Arabidopsis leaves: characterization of chlorophyll catabolites and of chlorophyll catabolic enzymes involved in the degreening reaction. *Plant Physiology, 139*, 52-63.

Qi, T. C., Wang, J. J., Huang, H., Liu, B., Gao, H., Liu, Y. L., et al. (2015). Regulation of jasmonate-induced leaf senescence by antagonism between bHLH subgroup IIIe and IIId factors in Arabidopsis. *The Plant Cell, 27*, 1634-1649.

Qiu, K., Li, Z., Yang, Z., Chen, J., Wu, S., Zhu, X., et al. (2015). EIN3 and ORE1 accelerate degreening during ethylene-mediated leaf senescence by directly activating chlorophyll catabolic genes in Arabidopsis. *PLoS Genetics, 11*, e1005399.

Raab, S., Drechsel, G., Zarepour, M., Hartung, W., Koshiba, T., Bittner, F., et al. (2009). Identification of a novel E3 ubiquitin ligase that is required for suppression of premature senescence in Arabidopsis. *The Plant Journal, 59*, 39-51.

Ren, G., An, K., Liao, Y., Zhou, X., Cao, Y., Zhao, H., et al. (2007). Identification of a novel chloroplast protein AtNYE1 regulating chlorophyll degradation during leaf senescence in Arabidopsis. *Plant Physiology, 144*, 1429-1441.

Ren, G. D., Zhou, Q., Wu, S. X., Zhang, Y. F., Zhang, L. G., Huang, J. R., et al. (2010). Reverse genetic identification of CRN1 and its distinctive role in chlorophyll degradation in *Arabidopsis*. *Journal of Integrative Plant Biology, 52*, 496-504.

Rios, J. J., Perez-Galvez, A., & Roca, M. (2014a). Non-fluorescent chlorophyll catabolites in quince fruits. *Food Research International, 65*, 255-262.

Rios, J. J., Roca, M., & Perez-Galvez, A. (2014b). Nonfluorescent chlorophyll catabolites in loquat fruits (*Eriobotrya japonica* Lindl.). *Journal of Agricultural and Food Chemistry, 62*, 10576-10584.

Roca, M., Rios, J. J., Chahuaris, A., & Perez-Galvez, A. (2017). Non-fluorescent and yellow chlorophyll catabolites in Japanese plum fruits (*Prunus salicina*, Lindl.). *Food Research International, 100*, 332-338.

Roca, M., Rios, J. J., & Perez-Galvez, A. (2018). Mass spectrometry: the indispensable tool for plant metabolomics of colourless chlorophyll catabolites. *Phytochemistry Reviews, 17*, 453-468.

Rodoni, S., Mühlecker, W., Anderl, M., Kräutler, B., Moser, D., Thomas, H., et al. (1997a). Chlorophyll breakdown in senescent chloroplasts. Cleavage of pheophorbide *a* in two enzymic steps. *Plant Physiology, 115*, 669-676.

Rodoni, S., Vicentini, F., Schellenberg, M., Matile, P., & Hörtensteiner, S. (1997b). Partial purification and characterization of red chlorophyll catabolite reductase, a stroma protein involved in chlorophyll breakdown. *Plant Physiology, 115*, 677-682.

Roiser, M. H., Müller, T., & Kräutler, B. (2015). Colorless chlorophyll catabolites in senescent florets of broccoli (*Brassica oleracea* var. italica). *Journal of Agricultural and Food Chemistry, 63*, 1385-1392.

Saga, Y., & Tamiaki, H. (2012). Demetalation of chlorophyll pigments. *Chemistry & Biodiversity, 9*, 1659-1683.

Sakuraba, Y., Han, S. H., Lee, S. H., Hörtensteiner, S., & Paek, N. C. (2016). *Arabidopsis* NAC016 promotes chlorophyll breakdown by directly upregulating *STAYGREEN1* transcription. *Plant Cell Reports, 35*, 155-166.

Sakuraba, Y., Jeong, J., Kang, M. Y., Kim, J., Paek, N. C., & Choi, G. (2014a). Phytochrome-interacting transcription factors PIF4 and PIF5 induce leaf senescence in Arabidopsis. *Nature Communications, 5*, 4636.

Sakuraba, Y., Kim, D., Kim, Y. S., Hörtensteiner, S., & Paek, N. C. (2014b). Arabidopsis STAYGREEN-LIKE (SGRL) promotes abiotic stress-induced leaf yellowing during vegetative growth. *FEBS Letters, 588*, 3830-3837.

Sakuraba, Y., Kim, Y. S., Yoo, S. C., Hörtensteiner, S., & Paek, N. C. (2013). 7-Hydroxymethyl chlorophyll *a* reductase functions in metabolic channeling of chlorophyll breakdown intermediates during leaf senescence. *Biochemical and Biophysical Research Communications, 430*, 32-37.

Sakuraba, Y., Schelbert, S., Park, S.-Y., Han, S.-H., Lee, B.-D., Besagni Andrès, C., et al. (2012). STAY-GREEN and chlorophyll catabolic enzymes interact at light-harvesting complex II for chlorophyll detoxification during leaf senescence in *Arabidopsis*. *The Plant Cell, 24*, 507-518.

Sato, Y., Moria, R., Katsuma, S., Nishimura, M., Tanaka, A., & Kusaba, M. (2009). Two short-chain dehydrogenase/reductases, NON-YELLOW COLORING 1 and NYC1-LIKE, are

required for chlorophyll *b* and light-harvesting complex II degradation during senescence in rice. *The Plant Journal, 57*, 120-131.

Sato, Y., Morita, R., Nishimura, M., Yamaguchi, H., & Kusaba, M. (2007). Mendel's green cotyledon gene encodes a positive regulator of the chlorophyll-degrading pathway. *Proceedings of the National Academy of Sciences, USA, 104*, 14169-14174.

Scheer, H. (2006). An overview of chlorophylls and bacteriochlorophylls: Biochemistry, biophysics, functions and applications. In B. Grimm, R. Porra, W. Rüdiger, & H. Scheer (Eds.), *Chlorophylls and Bacteriochlorophylls: Biochemistry, Biophysics, Functions and Applications* (Vol. 25, pp. 1-26). Dordrecht, The Netherlands: Springer.

Schelbert, S., Aubry, S., Burla, B., Agne, B., Kessler, F., Krupinska, K., et al. (2009). Pheophytin pheophorbide hydrolase (pheophytinase) is involved in chlorophyll breakdown during leaf senescence in Arabidopsis. *The Plant Cell, 21*, 767-785.

Scherl, M., Müller, T., & Kräutler, B. (2012). Chlorophyll catabolites in senescent leaves of the lime tree (*Tilia cordata*). *Chemistry & Biodiversity, 9*, 2605-2617.

Scherl, M., Müller, T., Kreutz, C. R., Huber, R. G., Zass, E., Liedl, K. R., et al. (2016). Chlorophyll catabolites in fall leaves of the wych elm tree present a novel glyosylation motif. *Chemistry - A European Journal, 22*, 9498-9503.

Scheumann, V., Schoch, S., & Rüdiger, W. (1999). Chlorophyll *b* reduction during senescence of barley seedlings. *Planta, 209*, 364-370.

Shan, X. Y., Wang, J. X., Chua, L. L., Jiang, D. A., Peng, W., & Xie, D. X. (2011). The role of Arabidopsis Rubisco activase in jasmonate-induced leaf senescence. *Plant Physiology, 155*, 751-764.

Shimoda, Y., Ito, H., & Tanaka, A. (2012). Conversion of chlorophyll *b* to chlorophyll *a* precedes magnesium dechelation for protection against necrosis in Arabidopsis. *The Plant Journal, 72*, 501-511.

Shimoda, Y., Ito, H., & Tanaka, A. (2016). Arabidopsis STAY-GREEN, Mendel's green cotyledon gene, encodes magnesium-dechelatase. *The Plant Cell, 28*, 2147-2160.

Sugishima, M., Kitamori, Y., Noguchi, M., Kohchi, T., & Fukuyama, K. (2009). Crystal structure of red chlorophyll catabolite reductase: enlargement of the ferredoxin-dependent bilin reductase family. *Journal of Molecular Biology, 389*, 376-387.

Sugishima, M., Okamoto, Y., Noguchi, M., Kohchi, T., Tamiaki, H., & Fukuyama, K. (2010). Crystal structures of the substrate-bound forms of red chlorophyll catabolite reductase: implications for site-specific and stereospecific reaction. *Journal of Molecular Biology, 402*, 879-891.

Süssenbacher, I., Christ, B., Hörtensteiner, S., & Kräutler, B. (2014). Hydroxymethylated phyllobilins: A puzzling new feature of the dioxobilin branch of chlorophyll breakdown. *Chemistry - A European Journal, 20*, 87-92.

Süssenbacher, I., Hörtensteiner, S., & Kräutler, B. (2015a). A dioxobilin-type fluorescent chlorophyll catabolite as a transient early intermediate of the dioxobilin-branch of chlorophyll breakdown in *Arabidopsis thaliana*. *Angewandte Chemie International Edition, 54*, 13777-13781.

Süssenbacher, I., Kreutz, C., Christ, B., Hörtensteiner, S., & Kräutler, B. (2015b). Hydroxymethylated dioxobilins in senescent *Arabidopsis thaliana* leaves - sign of a puzzling biosynthetic intermezzo of chlorophyll breakdown. *Chemistry - A European Journal, 21*, 11664-11670.

Suzuki, Y., Doi, M., & Shioi, Y. (2002). Two enzymatic reaction pathways in the formation of pyropheophorbide *a*. *Photosynthesis Research, 74*, 225-233.

Suzuki, Y., & Shioi, Y. (1999). Detection of chlorophyll breakdown products in the senescent leaves of higher plants. *Plant and Cell Physiology, 40*, 909-915.

Takasaki, H., Maruyama, K., Takahashi, F., Fujita, M., Yoshida, T., Nakashima, K., et al. (2015). SNAC-As, stress-responsive NAC transcription factors, mediate ABA-inducible leaf senescence. *The Plant Journal, 84*, 1114-1123.

Tanaka, A., & Tanaka, R. (2006). Chlorophyll metabolism. *Current Opinion in Plant Biology, 9*, 248-255.

Tanaka, R., Hirashima, M., Satoh, S., & Tanaka, A. (2003). The *Arabidopsis-accelerated cell death* gene *ACD1* is involved in oxygenation of pheophorbide *a*: inhibition of pheophorbide *a* oxygenase activity does not lead to the "stay-green" phenotype in *Arabidopsis*. *Plant and Cell Physiology, 44*, 1266-1274.

Tanaka, R., Kobayashi, K., & Masuda, T. (2011). Tetrapyrrole metabolism in *Arabidopsis thaliana*. *The Arabidopsis Book, 9*, e0145.

Tanaka, R., & Tanaka, A. (2011). Chlorophyll cycle regulates the construction and destruction of the light-harvesting complexes. *Biochimica et Biophysica Acta, 1807*, 968-976.

Thomas, H., Bortlik, K.-H., Rentsch, D., Schellenberg, M., & Matile, P. (1989). Catabolism of chlorophyll *in vivo*: significance of polar chlorophyll catabolites in a non-yellowing senescence mutant of *Festuca pratensis* Huds. *New Phytologist, 111*, 3-8.

Thomas, H., Huang, L., Young, M., & Ougham, H. (2009). Evolution of plant senescence. *BMC Evolutionary Biology, 9*, 163.

Tommasini, R., Vogt, E., Fromenteau, M., Hörtensteiner, S., Matile, P., Amrhein, N., et al. (1998). An ABC transporter of *Arabidopsis thaliana* has both glutathione-conjugate and chlorophyll catabolite transport activity. *The Plant Journal, 13*, 773-780.

Topalov, G., & Kishi, Y. (2001). Chlorophyll catabolism leading to the skeleton of dinoflagellate and krill luciferins: Hypothesis and model studies. *Angewandte Chemie International Edition, 40*, 3892-3894.

Ueda, J., & Kato, J. (1980). Isolation and identification of a senescence-promoting substance from wormwood (*Artemisia absinthium* L.). *Plant Physiology, 66*, 246-249.

Ulrich, M., Moser, S., Müller, T., & Kräutler, B. (2011). How the colourless 'nonfluorescent' chlorophyll catabolites rust. *Chemistry - A European Journal, 17*, 2330-2334.

Valenta, K., Kalbitzer, U., Razafimandimby, D., Omeja, P., Ayasse, M., Chapman, C. A., et al. (2018). The evolution of fruit colour: phylogeny, abiotic factors and the role of mutualists. *Scientific Reports, 8*, 14302.

Vergara-Dominguez, H., Rios, J. J., Gandul-Rojas, B., & Roca, M. (2016). Chlorophyll catabolism in olive fruits (var. Arbequina and Hojiblanca) during maturation. *Food Chemistry, 212*, 604-611.

Vergeiner, C., Banala, S., & Kräutler, B. (2013). Chlorophyll breakdown in senescent banana leaves: catabolism reprogrammed for biosynthesis of persistent blue fluorescent tetrapyrroles. *Chemistry - A European Journal, 19*, 12294-12305.

Vergeiner, C., Ulrich, M., Li, C. J., Liu, X. J., Müller, T., & Kräutler, B. (2015). Stereo- and regioselective phyllobilane oxidation in leaf homogenates of the peace lily (*Spathiphyllum wallisii*): hypothetical endogenous path to yellow chlorophyll catabolites. *Chemistry - A European Journal, 21*, 136-149.

Wakana, D., Kato, H., Momose, T., Sasaki, N., Ozeki, Y., & Goda, Y. (2014). NMR-based characterization of a novel yellow chlorophyll catabolite, Ed-YCC, isolated from *Egeria densa*. *Tetrahedron Letters, 55*, 2982-2985.

Wang, Y. Q., Yang, Y., Fei, Z. J., Yuan, H., Fish, T., Thannhauser, T. W., et al. (2013). Proteomic analysis of chromoplasts from six crop species reveals insights into chromoplast function and development. *Journal of Experimental Botany, 64*, 949-961.

Wilks, A. (2008). Heme degradation : mechanistic and physiological implications. In M. J. Warren & A. G. Smith (Eds.), *Tetrapyrroles: Birth, Life and Death* (pp. 101-115). Austin, Texas: Landes Bioscience.

Wilks, A., & Ikeda-Saito, M. (2014). Heme utilization by pathogenic bacteria: not all pathways lead to biliverdin. *Accounts of Chemical Research, 47*, 2291-2298.

Wu, S., Li, Z., Yang, L., Xie, Z., Chen, J., Zhang, W., et al. (2016). NON-YELLOWING2 (NYE2), a close paralog of NYE1, plays a positive role in chlorophyll degradation in Arabidopsis. *Molecular Plant, 9*, 624-627.

Wüthrich, K. L., Bovet, L., Hunziker, P. E., Donnison, I. S., & Hörtensteiner, S. (2000). Molecular cloning, functional expression and characterisation of RCC reductase involved in chlorophyll catabolism. *The Plant Journal, 21*, 189-198.

Xodo, L. E., Rapozzi, V., Zacchigna, M., Drioli, S., & Zorzet, S. (2012). The chlorophyll catabolite pheophorbide *a* as a photosensitizer for the photodynamic therapy. *Current Medicinal Chemistry, 19*, 799-807.

Yang, Y., Xu, R., Ma, C. J., Vlot, A. C., Klessig, D. F., & Pichersky, E. (2008). Inactive methyl indole-3-acetic acid ester can be hydrolyzed and activated by several esterases belonging to the *At*MES esterase family of Arabidopsis. *Plant Physiology, 147*, 1034-1045.

Ye, Y., Zhou, L., Liu, X., Liu, H., Li, D., Cao, M., et al. (2017). A novel chemical inhibitor of ABA signaling targets all ABA receptors. *Plant Physiology, 173*, 2356-2369.

Yin, X. R., Xie, X. L., Xia, X. J., Yu, J. Q., Ferguson, I. B., Giovannoni, J. J., et al. (2016). Involvement of an ethylene response factor in chlorophyll degradation during citrus fruit degreening. *The Plant Journal, 86*, 403-412.

Zapata, L., Ding, J., Willing, E. M., Hartwig, B., Bezdan, D., Jiao, W. B., et al. (2016). Chromosome-level assembly of *Arabidopsis thaliana* L*er* reveals the extent of translocation and inversion polymorphisms. *Proceedings of the National Academy of Sciences, USA, 113*, E4052-4060.

Zhang, J., Yu, G., Wen, W., Ma, X., Xu, B., & Huang, B. (2016). Functional characterization and hormonal regulation of the *PHEOPHYTINASE* gene *LpPPH* controlling leaf senescence in perennial ryegrass. *Journal of Experimental Botany, 67*, 935-945.

Zhang, W., Liu, T. Q., Ren, G. D., Hörtensteiner, S., Zhou, Y. M., Cahoon, E. B., et al. (2014). Chlorophyll degradation: the tocopherol biosynthesis related phytol hydrolase in Arabidopsis seeds is still missing. *Plant Physiology, 166*, 70-79.

Zhu, X., Chen, J., Xie, Z., Gao, J., Ren, G., Gao, S., et al. (2015). Jasmonic acid promotes degreening via MYC2/3/4- and ANAC019/055/072-mediated regulation of major chlorophyll catabolic genes. *The Plant Journal, 84*, 597-610.

Zhu, X. Y., Chen, J. Y., Qiu, K., & Kuai, B. K. (2017). Phytohormone and light regulation of chlorophyll degradation. *Frontiers in Plant Science, 8*, 1911.

Figure legend

Figure 1. Topology of the PAO/phyllobilin pathway of chlorophyll breakdown. Chl degradation starts at the thylakoid membrane of the senescing chloroplast. *p*FCC and/or 3^2-hydroxy-*p*FCCs ('secondary' FCCs; *s*FCCs) produced by TIC55 are exported from the plastid to the cytosol by unknown transporter(s). In the cytosol, side chain modifications may occur that lead to the formation of 'modified' FCCs (*m*FCCs) or of DFCCs when involving the action of ER-localized CYP89A9. Modified fluorescent phyllobilins (*m*FCCs and DFCCs) are then imported into the vacuole by unknown transporter(s), where they are converted to respective nonfluorescent isomers (NCCs and DNCCs) due to the acidic milieu. NCCs (DNCCs) may further be converted to YCCs (DYCCs) and PiCCs (DPiCCs). For abbreviations, see text and list of abbreviations.